Refractive Index Measurements of Films with Biaxial Symmetry. 1. Determination of Complex Refractive Indices Using Polarized Reflectance/Transmittance Ratio

Jie Diao and Dennis W. Hess*

School of Chemical and Biomolecular Engineering, Georgia Institute of Technology, Atlanta, Georgia 30332-0100

Received: August 18, 2004; In Final Form: May 4, 2005

A new method to extract complex refractive indices of films with biaxial symmetry from polarized transmission and reflection spectra is described. Theoretical analysis demonstrates that the reflectance/transmittance ratio (R/T ratio) of two films of different thicknesses but with the same optical anisotropy is a simple function of the refractive index (n) and extinction coefficient (k). For films with biaxial symmetry, components of n and k on symmetric axes can be extracted from either s- or p-polarized R/T ratios if the film thickness values are known. The R/T ratio method can generate n and k spectra within a particular wavelength range without assuming a specific relationship among n, k, and wavelength, which is an advantage over many currently available techniques. The R/T ratio method is used to extract the anisotropic complex refractive indices of a polyimide film with known uniaxial symmetry. The resultant n and k spectra compare well with simulations based on known n and k values. The accuracy of n and k spectra is affected mostly by data error in reflection and transmission spectra collection, thickness variation across sample films, and error in sample alignment.

1. Introduction

Considerable interest exists in experimentally determining the refractive index (n) and the extinction coefficient (k), or complex refractive index ($n - ik$), of biaxially or uniaxially symmetric films.[1−6] The directional dependence of the optical properties can provide useful information on molecular orientation in films.[1] Several techniques are currently available to determine anisotropic complex refractive indices of thin films such as prism coupling techniques,[2] spectroscopic ellipsometry,[1,3,4] attenuated total reflection spectroscopy (ATR),[5] and methods based on transmission and reflection spectra.[6]

In prism coupling measurements, a thin film is contacted with a prism and the reflected intensity of light through the prim changes with incident angle as a result of guided propagation of light in the thin film. The dependence of reflectivity on incident angle of s- and p-polarized light can be used to derive anisotropic n and k values.[2] In spectroscopic ellipsometry, the difference in the phase of reflected or transmitted s- and p-polarized light and the ratio between the changes in amplitude are measured, and the anisotropic n and k are obtained by fitting the simulated data to the measured values.[8,9] In data fitting, a model describing the relation between n, k, and the wavelength is usually assumed.[3,4,7,8] In ATR spectroscopy, n and k are calculated from the reflectivity data under total reflection mode. A model describing the relation among n, k, and the wavelength must be assumed.[5] In addition to the above techniques, methods that use transmission or reflection spectra to extract anisotropic complex refractive indices will be of special interest since collection of transmission and reflection spectra is routine in many laboratories. For instance, a procedure has been developed to obtain the in-plane and out-of-plane refractive indices of a uniaxially oriented film from a normalized transmission spectrum at normal incidence and a p-polarized reflection spectrum at grazing incidence, respectively.[6] The procedure used a matrix formalism to simulate spectra of anisotropic multilayer systems and the Kramers−Kronig relationship to describe the interdependence of n and k. The film thickness was obtained from spectroscopic ellipsometry measurements and was subsequently used in the spectral simulation.[6]

The prism coupling technique can be used to extract n and k without assuming a relationship between n and k. However, it is limited to the extraction of n and k at specific laser wavelengths such as 632.8, 1550 nm, etc. Although other methods can generate continuous n and k spectra over a wavelength range, they generally require an assumed relationship between n and k, which demands preliminary knowledge about the physics of the film. In this paper, a new reflectance/transmittance ratio method is proposed to extract the complex refractive indices of absorbing free-standing films with biaxial symmetry from transmission and reflection spectra at oblique incidence. This method can generate the complex refractive index spectra from a series of films of different thicknesses but with the same optical anisotropy. No pre-assumed relation between n and k is required.

2. Theory

Extraction of complex refractive indices from reflectance/transmittance (R/T) data is based on the 4×4 transfer matrix method; details of this transfer matrix method can be found elsewhere[9,10] and are not provided here. To aid the readers, we use nomenclature consistent with that in refs 9 and 10. For clarity and conciseness, we begin the development with some expressions that are derived in detail in Appendix I. The transfer matrix method is applicable to multilayer film structures with any total number (N) of layers, each of which has a degree of anisotropy up to and including full biaxial symmetry.[9] The value of a variable such as V, in a specific layer (e.g., i), is denoted as $V(i)$. V can be a scalar, a vector, or a tensor. If V is not followed by a cardinal number, it means the designation is

* Corresponding author. Tel.: +1-404-894-5922. Fax: +1-404-894-2866. E-mail: dennis.hess@chbe.gatech.edu.

10.1021/jp046277t CCC: $30.25
Published on Web 06/10/2005

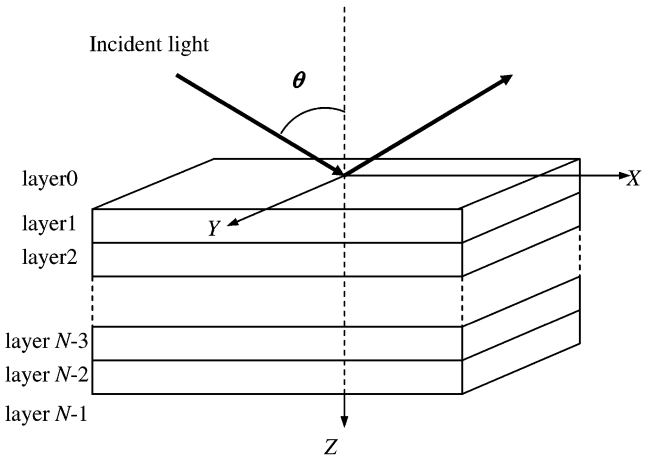

(a) Total number of layers=*N*

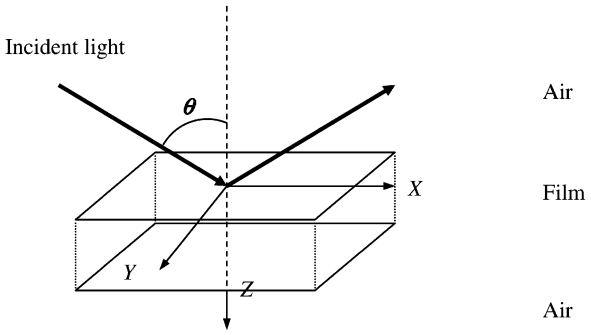

(b) A freestanding film in air (*N*=3)

Figure 1. Geometry of electromagnetic wave propagation: (a) Total number of layers = *N*; (b) A free-standing film in air (*N* = 3).

applicable to all layers. |⋯| will be used to denote the modulus of a complex vector or number in this paper.

According to the matrix method, for a layered structure containing a total of *N* semi-infinite (in *XY* plane), parallel and planar layers of definite thickness stacked in the *Z* direction (Figure 1a), the electric fields in the final medium ($N - 1$) and the first medium (0) are related by the following equation:

$$\begin{pmatrix} A_1(0) \\ A_2(0) \\ A_3(0) \\ A_4(0) \end{pmatrix} = \mathbf{M} \begin{pmatrix} A_1(N-1) \\ A_2(N-1) \\ A_3(N-1) \\ A_4(N-1) \end{pmatrix} \tag{1}$$

In the equation (eq 1), A_1, A_2, A_3, and A_4 are complex amplitudes of the electromagnetic waves and are arranged in a sequence such that A_1 corresponds to the wave propagating in the positive *Z* direction with a zero *Y* component of **p** (forward p-polarized wave), A_2 to the wave propagating in the negative *Z* direction with a zero *Y* component of **p** (backward p-polarized wave), A_3 to the wave propagating in the positive *Z* direction with a zero *XZ* component of **p** (forward s-polarized wave), and A_4 to the wave propagating in the negative *Z* direction with a zero *XZ* component of **p** (backward s-polarized wave). The definition of **p** can be found in Appendix I. **M** is known as the transfer matrix. Because there will be no backward waves in the last layer, $A_2(N - 1) = A_4(N - 1) = 0$.

For a system consisting only of a free-standing film in air, the total number of layers, *N*, will be 3, and $A_1(0)$, $A_2(0)$, and $A_1(2)$ will be the complex amplitudes of the incident, reflected and transmitted p-polarized light, respectively; $A_3(0)$, $A_4(0)$, and $A_3(2)$ will be the complex amplitudes of the incident, reflected and transmitted s-polarized light, respectively. Transmittance (T_p) and reflectance (R_p) of p-polarized light can be calculated from[9]

$$T_p = \frac{|A_1(2)|^2}{|A_1(0)|^2} \tag{2}$$

$$R_p = \frac{|A_2(0)|^2}{|A_1(0)|^2} \tag{3}$$

Similarly, transmittance (T_s) and reflectance (R_s) of s-polarized light can be calculated from

$$T_s = \frac{|A_3(2)|^2}{|A_3(0)|^2} \tag{4}$$

$$R_s = \frac{|A_4(0)|^2}{|A_3(0)|^2} \tag{5}$$

In the following, we assume that the film is absorbing and is biaxial (with the symmetry axes coinciding with *X*, *Y*, and *Z* axes) and use n_x, n_y, and n_z and k_x, k_y, and k_z to denote the *X*, *Y*, and *Z* components of *n* and *k*, respectively. Let n_0 be the refractive index of air, *t* the film thickness, ω the frequency of incident light, and *c* the speed of light in a vacuum. If the light is incident from vacuum (or air) in the *XZ* plane with an incident angle of θ (Figure 1b), T_p and R_p can be calculated from the following two equations (Appendix I):

$$1/T_p = \left|\left(\frac{1}{2} + \frac{H}{4} + \frac{1}{4H}\right)\exp[i\gamma_1(1)t] + \left(\frac{1}{2} - \frac{H}{4} - \frac{1}{4H}\right) \times \exp[-i\gamma_1(1)t]\right|^2 \tag{6}$$

$$1/R_p = \left|\frac{\left(\frac{1}{2} + \frac{H}{4} + \frac{1}{4H}\right)\exp[i\gamma_1(1)t] + \left(\frac{1}{2} - \frac{H}{4} - \frac{1}{4H}\right)\exp[-i\gamma_1(1)t]}{\left(\frac{H}{4} - \frac{1}{4H}\right)\exp[i\gamma_1(1)t] - \left(\frac{H}{4} - \frac{1}{4H}\right)\exp[-i\gamma_1(1)t]}\right|^2 \tag{7}$$

where

$$H = \frac{{n_0}^2\sqrt{(n_z - ik_z)^2 - \sin^2\theta}}{(n_x - ik_x)(n_z - ik_z)\sqrt{{n_0}^2 - \sin^2\theta}} \tag{8}$$

and

$$\gamma_1(1) = (\omega/c)\frac{(n_x - ik_x)}{(n_z - ik_z)}\sqrt{(n_z - ik_z)^2 - \sin^2\theta} \tag{9}$$

Likewise, T_s and R_s can be calculated from the following two equations:

$$1/T_s = \left|\left(\frac{1}{2} + \frac{G}{4} + \frac{1}{4G}\right)\exp[i\gamma_3(1)t] + \left(\frac{1}{2} - \frac{G}{4} - \frac{1}{4G}\right) \times \exp[-i\gamma_3(1)t]\right|^2 \tag{10}$$

$$1/R_s = \left| \frac{\left(\frac{1}{2} + \frac{G}{4} + \frac{1}{4G}\right)\exp[i\gamma_3(1)t] + \left(\frac{1}{2} - \frac{G}{4} - \frac{1}{4G}\right)\exp[-i\gamma_3(1)t]}{\left(\frac{G}{4} - \frac{1}{4G}\right)\exp[i\gamma_3(1)t] - \left(\frac{G}{4} - \frac{1}{4G}\right)\exp[-i\gamma_3(1)t]} \right|^2 \quad (11)$$

where

$$G = \frac{\sqrt{{n_0}^2 - \sin^2\theta}}{\sqrt{(n_y - ik_y)^2 - \sin^2\theta}} \quad (12)$$

and

$$\gamma_3(1) = (\omega/c)\sqrt{(n_y - ik_y)^2 - \sin^2\theta} \quad (13)$$

The ratios between R and T for p- and s-polarized light can be expressed as

$$R_p/T_p = \left|\left(\frac{H}{4} - \frac{1}{4H}\right)\right|^2 \cdot |\exp[i\gamma_1(1)t] - \exp[-i\gamma_1(1)t]|^2 \quad (14)$$

and

$$R_s/T_s = \left|\left(\frac{G}{4} - \frac{1}{4G}\right)\right|^2 \cdot |\exp[i\gamma_3(1)t] - \exp[-i\gamma_3(1)t]|^2 \quad (15)$$

respectively. For two films of different thicknesses (t_1 and t_2) but with the same optical anisotropy, identical H, G, and γ values occur for the same incident angle. Therefore

$$\frac{(R_p/T_p)_{t=t_1}}{(R_p/T_p)_{t=t_2}} = \frac{|\exp[i\gamma_1(1)t_1] - \exp[-i\gamma_1(1)t_1]|^2}{|\exp[i\gamma_1(1)t_2] - \exp[-i\gamma_1(1)t_2]|^2} \quad (16)$$

and

$$\frac{(R_s/T_s)_{t=t_1}}{(R_s/T_s)_{t=t_2}} = \frac{|\exp[i\gamma_3(1)t_1] - \exp[-i\gamma_3(1)t_1]|^2}{|\exp[i\gamma_3(1)t_2] - \exp[-i\gamma_3(1)t_2]|^2} \quad (17)$$

$\gamma_3(1)$ is a complex number and contains both real and imaginary parts. The equation (eq 17) can be used to calculate $\gamma_3(1)$ if s-polarized reflection and transmission spectra of three films with known but different thicknesses (two R/T ratios) are available. As the value of $\gamma_3(1)$ is determined, n_y and k_y can be calculated from eq 13. In addition, n_x and k_x values can be calculated from the s-polarized reflection and transmission spectra when the sample film is rotated 90° about the Z axis. Similarly, $\gamma_1(1)$ can be obtained from reflection and transmission spectra of p-polarized light. If n_x, k_x are already known, n_z and k_z can be calculated from eq 9. To improve the accuracy of calculated n and k values, polarized reflection and transmission spectra of more than three films (all with different thicknesses but with the same optical anisotropy) can be collected and γ can be obtained by data fitting with known values of $||\exp[i\gamma t_1] - \exp[-i\gamma t_1]||/||\exp[i\gamma t_m] - \exp[-i\gamma t_m]||$, $m = 2, 3$, etc. In practice, the step of obtaining γ values can be eliminated; n and k values can be generated directly from the data fitting process. In the following discussions, this method of obtaining n and k when t is known will be designated R/T ratio method.

Since the R/T ratio method uses the light intensity ratio, error resulting from incident light scattering is reduced because it is expected that the loss of intensity due to scattering will influence both the reflected and the transmitted light intensities in a similar manner. This fact also implies that the method does not require an accurate background for reflection spectra since intensities are ratioed. In practice, to obtain sufficiently accurate absolute reflection spectra, either a calibrated mirror (which may have a short shelf life) or a carefully designed experimental configuration is required.[12] In addition, effects caused by absorption of atmospheric water and carbon dioxide will not cause significant error provided that the humidity and CO_2 content in the air do not change significantly during data collection. Therefore, purging or evacuation of the sample chamber is not required.

However, the primary advantage of the R/T ratio method is that no model or relationship for n and k is needed to calculate n and k spectra; this distinguishes the R/T ratio method from other methods currently used on thin solid films. Implementation of the method requires that the three principal axes of the dielectric function (Appendix I) can be identified without ambiguity and that one of the principal axes must be normal to the film surface (in the Z direction) with the remaining two in the X and Y directions, respectively. In addition, a series of free-standing films with different thicknesses but with the same anisotropy must be available. Caution must be exercised if thick films are used. For instance, if the films are nearly transparent in the wavelength range, the spectrometer may not resolve dense interference patterns in the transmission and reflection spectra when the films are more than 100 μm thick; if the films are absorbing in the wavelength range, the film should never be so thick that the intensity of transmitted or reflected light is below the detection limit of the spectrometer.

Since it has been widely reported that spin-coated poly(biphenyl dianhydride-*p*-phenylenediamine) (BPDA-PDA) polyimide films exhibit uniaxial optical anisotropy,[12−15] the R/T ratio method is used in this study to obtain the anisotropic complex refractive indices of BPDA-PDA films in the infrared range.

3. Experimental Procedures

3.1. Film Preparation. BPDA-PDA (PI2611) was obtained from HD Microsystems, Inc., in the poly(amic acid) form dissolved in *N*-methyl pyrrolidone (NMP); this solution was used as received. A 3000 Å Cr layer was first deposited on the front (smooth) side of a four-inch silicon wafer. Then the front side of the silicon wafer was spin coated (3000rpm) with an adhesion promoter (VM652 from HD Microsystems, Inc.) and heated on a hot plate at 110 °C for 1 min, followed by poly (amic acid) spin coating at 5000 rpm. The film was soft baked at 90 °C for 1.5 min and hard baked at 150 °C for 1.5 min to remove most of the NMP solvent, followed by a curing process in nitrogen at 350 °C for 30 min with a temperature ramp rate of 4 °C/min. A silicon etching mask layer (~3 μm cured BPDA-PDA on top of 3000 Å DC sputtered Cr layer) was deposited on the back (rough) side of the silicon wafer. Then the front (polyimide) side of the wafer was protected by spin coating a thin layer of photoresist (AZ P4620 from Clariant, Inc.). One-centimeter diameter circular openings were fabricated on the silicon etching mask layer by photolithographic patterning. In the photolithographic patterning, PR1827 from Shipley, Inc., served both as photoresist and etching mask for BPDA-PDA dry etch and Cr wet tech. BPDA-PDA dry etch was conducted in a Plasma-Therm reactive ion etcher with an 11-in. electrode. The etching gas was a mixture of CHF_3 (5 sccm) and O_2 (45 sccm). The etching was performed at 34 °C, 200 mTorr, and an RF power of 350 W. Cr was wet etched in a commercial Cr etchant (CR-7S from Cyantek, Inc.). Subsequently, a 1:1:1 mixture of 49% (w.t.) HF and 70% (w.t.) HNO_3 and deionized (DI) water was used to etch silicon from the backside in the open circular areas.

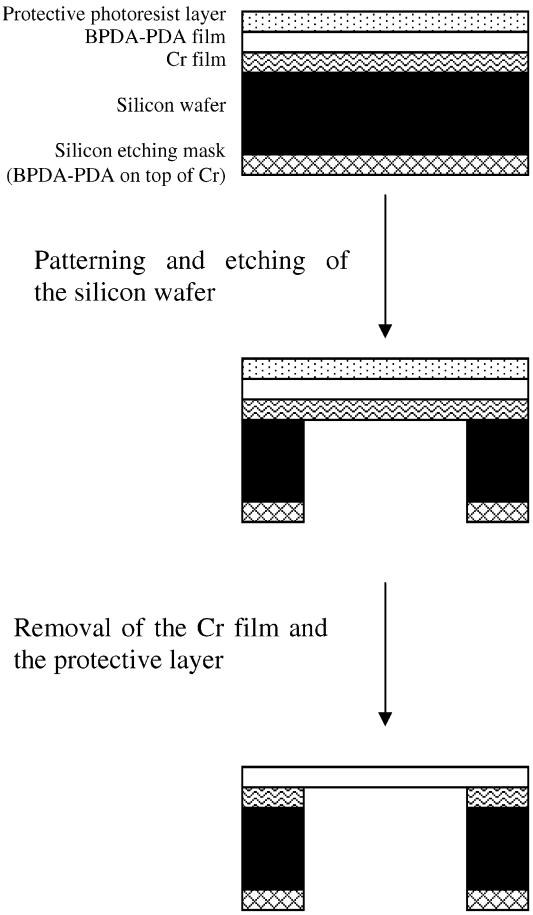

Figure 2. Fabrication of a free-standing BPDA-PDA film.

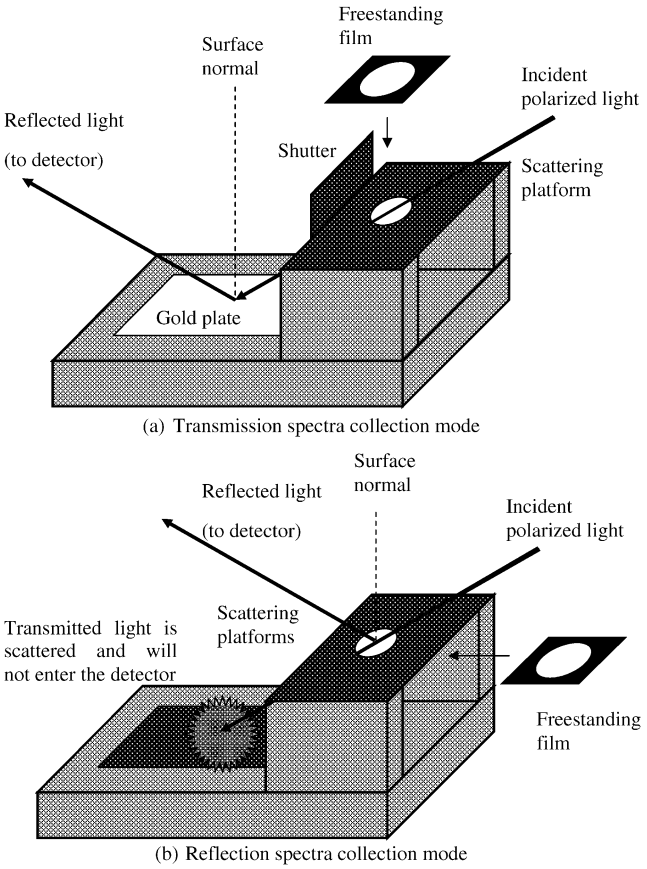

Figure 3. Two different operation modes for the FTIR reflection configuration: (a) Transmission spectra collection mode; (b) reflection spectra collection mode.

The layer of 3000 Å DC sputtered Cr, which is inert to the HF + HNO_3 mixture, between the front side BPDA-PDA film and the silicon wafer, served to isolate the HF + HNO_3 mixture from the front side BPDA-PDA film during silicon wet etching. After silicon was etched away in the open areas, the Cr layer was removed using CR-7S. Thus, the BPDA-PDA films in the open areas became free-standing. Finally, the front-side photoresist layer was removed using acetone. Figure 2 schematically shows the free-standing film fabrication process. FTIR spectra reveal no detectable change of BPDA-PDA films due to treatment by either acetone or CR-7S.

The free-standing BPDA-PDA films were dry-etched in the Plasma-Therm reactive ion etcher using the same etch gases and conditions described above. Etching for different times produced a series of films with the same optical anisotropy but with different thicknesses.[15] The surface roughness of BPDA-PDA films after reactive ion etching was ∼15 nm.[15]

3.2. FTIR Measurements. Infrared spectra were collected with a Bruker Equinox 55 infrared spectrometer equipped with a deuterated triglycine sulfide (DTGS) detector. All spectra were taken at 2 cm^{-1} resolution, 512 scans in the wavelength range of 400∼6000 cm^{-1}. The polarization state of incident light was adjusted by using both a Harrick KRS-5 wire grid polarizer and a Perkin-Elmer wire grid polarizer; two polarizers were used side-by-side in series to increase the polarization efficiency. A variable angle reflection stage was modified to allow switching between transmission and reflection spectra collection modes (Figure 3). In the transmission spectra collection mode, incident light passed through a circular optical aperture (8 mm in diameter) on a scattering platform and was reflected by a specular gold plate before entering the detector. Transmission background spectra were collected without the free-standing film on the optical aperture. The scattering platform was fabricated by using a piece of sand paper to scatter light outside the optical aperture area. In this way, the sampling area can be strictly controlled. A small shutter is placed in the path of light reflected by the film to prevent the light from entering the detector. In the reflection spectra collection mode, the free-standing film was positioned immediately below the scattering platform. Incident light in the optical aperture area was reflected by the film and entered the detector. Transmitted light hit the scattering platform and was scattered. Reflection background spectra were collected by replacing the free-standing film with the specular gold plate. Particular care was exercised in optical alignment to ensure that identical area on a film was sampled when switching from transmission mode to reflection mode.

4. Data Analysis

When applying the R/T ratio method, the film thickness must be known. Although film thickness can be determined by numerous methods, the thickness value should be obtained by a method in which the entire illuminated area is used in thickness determination. Previous ultraviolet−visible (UV−vis) and infrared (IR) absorption studies have indicated that BPDA-PDA films are transparent in the wavelength range between 1.5 and 2.5 μm (corresponding to ∼6600−4000 cm^{-1}) and show little dispersion in refractive index.[13] Therefore, we extended the total wavelength range to the near-infrared (up to 6000 cm^{-1}, which is the upper limit of the spectrometer) for infrared spectra collection and used the transmission spectra between 4500 and 6000 cm^{-1} to extract the film thickness. The wavelength range between 4000 and 4500 cm^{-1} was excluded to minimize the

TABLE 1: Film Pairing Used for R/T Ratio Calculation with Spectra Collected at 45° Incident Angle[a]

sequence number of film pair, l	t_{al}, μm	t_{bl}, μm
1	3.50 (3.47)	1.79 (1.80)
2	3.32 (3.28)	2.36 (2.30)
3	2.89 (2.81)	2.36 (2.30)
4	2.36 (2.30)	1.79 (1.80)

[a] Values in parentheses are the values used for calculations with spectra collected at 56° incident angle.

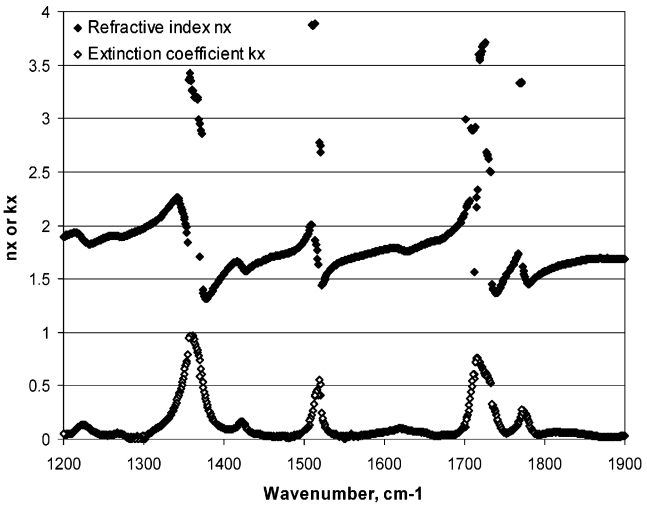

(a) n_x and k_x

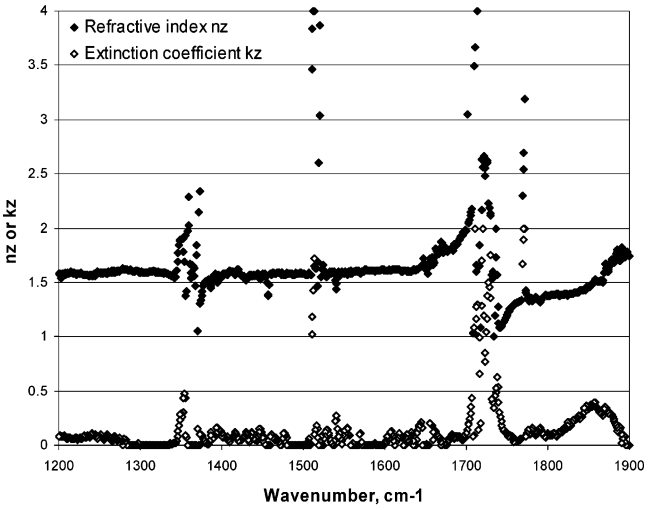

(b) n_z and k_z

Figure 4. n and k spectra extracted from R/T ratios at 45° incident angle (no points excluded): (a) n_x and k_x; (b) n_z and k_z.

influence of water vapor absorption near 4000 cm^{-1}. A detailed description of the thickness determination of transparent anisotropic films using polarized transmission spectra is published elsewhere.[16] Theoretically, only R and T at three different thicknesses, corresponding to two different thickness pairs, are required to calculate n and k. However, because both reflectance and transmittance can be close to zero due to either film absorption or interference, R/T ratios may involve a small number in the denominator at some wavelengths, which can introduce significant errors into the calculated n and k values. To ensure more accurate results, R and T spectra at five different thicknesses were collected so that R/T ratios with four independent thickness pairs can be used to determine n and k.

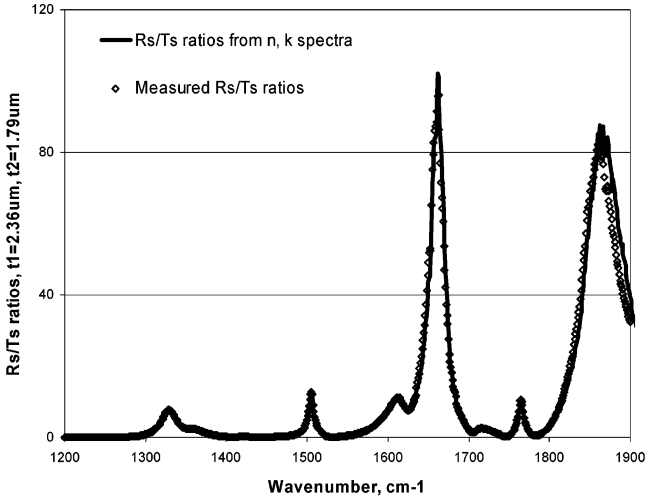

(a) R/T ratios for s-polarized light (t_1=2.36μm, t_2=1.79μm)

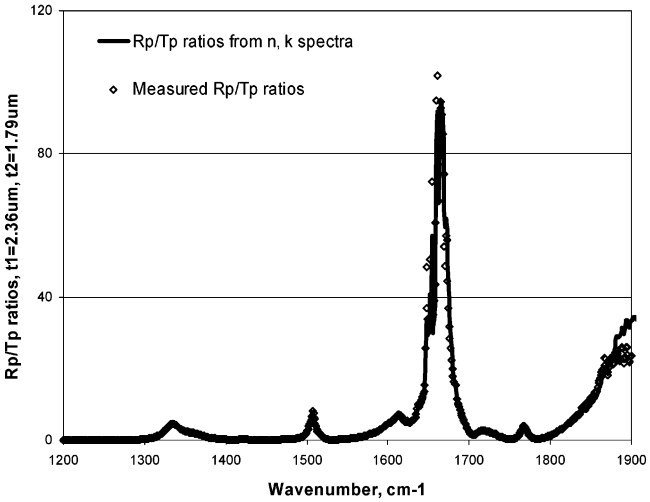

(b) R/T ratios for s-polarized light (t_1=2.36μm, t_2=1.79μm)

Figure 5. Comparison between measured R/T ratios and R/T ratios generated from the n and k spectra in Figure 4: (a) R/T ratios for s-polarized light (t_1 = 2.36 μm, t_2 = 1.79 μm); (b) R/T ratios for s-polarized light (t_1 = 2.36 μm, t_2 = 1.79 μm).

Optimal n and k values are determined by minimizing the following target function $g(n,k)$:

$$g(n,k) = \sum_{l=1}^{4}\left(\frac{(R/T)_{a_l,\text{measured}}/(R/T)_{b_l,\text{measured}}}{|\exp(i\gamma t_{a_l}) - \exp(-i\gamma t_{a_l})|^2/|\exp(i\gamma t_{b_l}) - \exp(-i\gamma t_{b_l})|^2} - 1\right)^2 \quad (18)$$

where l is the sequence number of the thickness pairs, and a_l and b_l denote the first film and second film in the lth pair. $\gamma = \gamma_1$ for p-polarized light; $\gamma = \gamma_3$ for s-polarized light. For five films of different thicknesses, there are many possible pair combinations. To reduce experimental error, pairings that give the largest ranges for $(R/T)_{al,\text{measured}}/(R/T)_{bl,\text{measured}}$ at most wavelengths should be chosen. Table 1 lists the film pairs used to calculate R/T ratios in this paper.

With four R/T ratios, a search for n and k can be performed by any classic minimum searching method, such as the simplex method[17] in a Matlab 6.x function "fminsearch". An initial guess of n and k must be supplied at each wavelength for the simplex method. Because both n and k are continuous functions with respect to wavelength, n and k values obtained at a particular

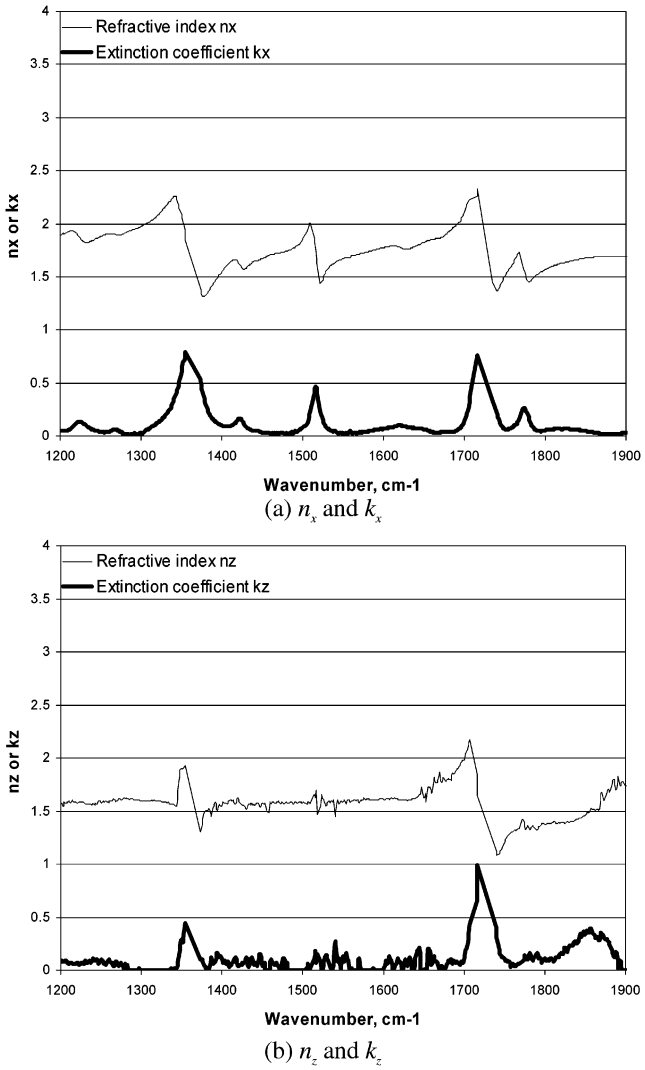

Figure 6. *n* and *k* spectra extracted from R/T ratios at 45° incident angle (discontinuous points excluded): (a) n_x and k_x; (b) n_z and k_z.

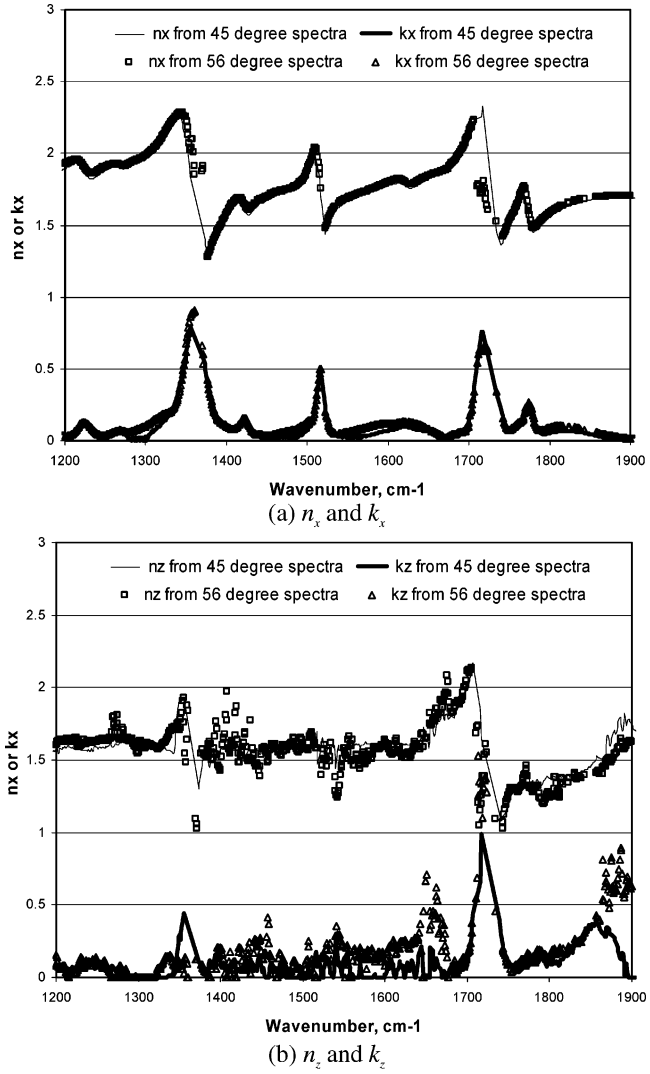

Figure 7. Comparison between n and k spectra extracted from R/T ratios at 45° incident angle and R/T ratios at 56° degree incident angle (discontinuous points excluded): (a) n_x and k_x; (b) n_z and k_z.

wavelength will be a viable initial guess for *n* and *k* calculation at an adjacent wavelength. However, in practice, we have found that use of *n* and *k* values at an adjacent wavelength as initial guesses does not yield stable iteration. If the results at one wavelength are incorrect due to measurement error, an incorrect initial guess will be entered into the calculation at the next wavelength and this may cause the search algorithm to converge at incorrect *n* and *k* values, which will be supplied as the initial guess for the next wavelength. The domino effect makes the algorithm unstable. In our calculations, we use a primitive searching scheme described as follows. Because both *n* and *k* are expected to fall in well-defined ranges, such as $n \in [0, 4]$ and $k \in [0, 2]$, we determine the optimal *n* and *k* values by meshing the rectangle representing $[0 \leq n \leq 4, 0 \leq k \leq 2]$ on the *nk* plane and finding the mesh point that gives the smallest $g(n,k)$. Computationally, both *n* and *k* were increased at a step size of 0.002. Thus at each wavelength, $g(n,k)$ was evaluated and compared for 2.0×10^6 times. The computation was not particularly intensive such that a desktop computer equipped with a 1.7 GHz processor and 512M random access memory (RAM) yielded results in ~12 h for the spectral range 1000~2000 cm^{-1} with a resolution of 2 cm^{-1}. Compared with the simplex searching algorithm, the algorithm we used was slower but more stable. Due to experimental error, at some wavelength, the resulting *n* and *k* show scatter from adjacent *n* and *k* points. Because both *n* and *k* should be continuous functions of wavelength with no abrupt change in values, *n* and

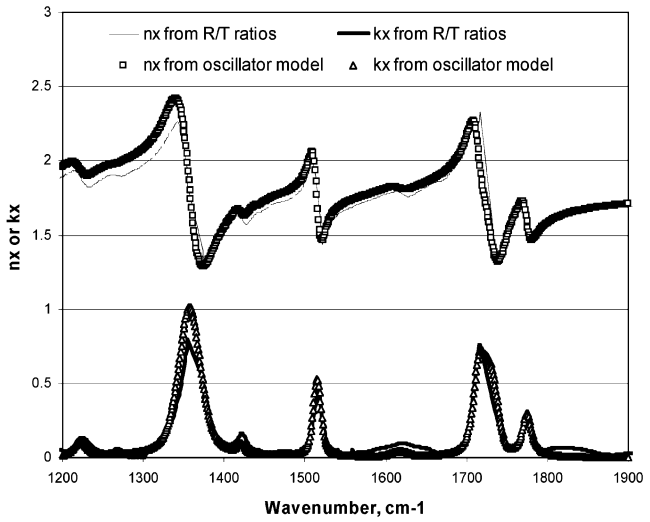

Figure 8. Comparison between n and k spectra extracted from R/T ratios at 45° incident angle and those generated from simulation based on an oscillator model.[18,19]

TABLE 2: Film Pairing Used for Simulation Study on the Influence of Thickness Variation

sequence number of film pair, l	t_{al}, μm	t_{bl}, μm
(a) The Case of Three Films		
1	3.0	2.4
2	2.4	1.8
(b) The Case of Five Films		
1	3.0	2.7
2	2.7	2.4
3	2.4	2.1
4	2.1	1.8

k values that caused apparent discontinuities are excluded from final n and k plots.

5. Results and Discussion

5.1. n and k Spectra Extracted from R/T Ratios at 45° Incident Angle. Figure 4 shows the n and k spectra extracted from R/T ratios calculated from reflection and transmission spectra collected at 45° incident angle. The wavelength range of 1200−1900 cm^{-1} is chosen for convenience in comparing results with literature values (see below). Scattering of n and k values is evident in the absorbing wavelength range. As discussed above, scattering is expected because in the absorbing wavelength range, either T or R (or both) will become very small due to film absorption; the detection error for weak signals can increase and a small numerical value on the denominator in R/T can cause large errors. It is also obvious that the data scattering is more serious for n_z and k_z relative to n_x and k_x. Since n_x and k_x are supplied as known values when calculating n_z and k_z using eq 9, any calculation error in n_x and k_x will propagate to n_z and k_z.

Figure 5 compares R/T ratios reconstructed from the n and k spectra in Figure 4 to experimentally measured R/T ratios. To make the figures easier to view, only the R/T ratio from one thickness pair ($t_1 = 2.36\mu$m, $t_2 = 1.79\mu$m) is shown. The match between reconstructed and measured R/T ratios is generally excellent. Again, because R_s/T_s ratios are determined solely by n_x and k_x while R_p/T_p ratios are functions of n_x, k_x, n_z, and k_z, it is apparent that the match is not as good for R_p/T_p ratios.

As mentioned in the Data Analysis section, both n and k should be continuous functions of wavelength and no abrupt change in their values is expected. Thus, n and k values that cause apparent discontinuities are deleted from the n and k plots. Figure 6 shows the resultant n and k spectra after these discontinuous points are excluded from Figure 4. Consistent with the data in Figure 5, n_z and k_z also show more scattering in Figure 6.

5.2. n and k Spectra Extracted from R/T Ratios at 56° Incident Angle. Reflection and transmission spectra were also collected at an incident angle of 56° and were used to calculate n and k spectra. The same thickness pairings were used as for

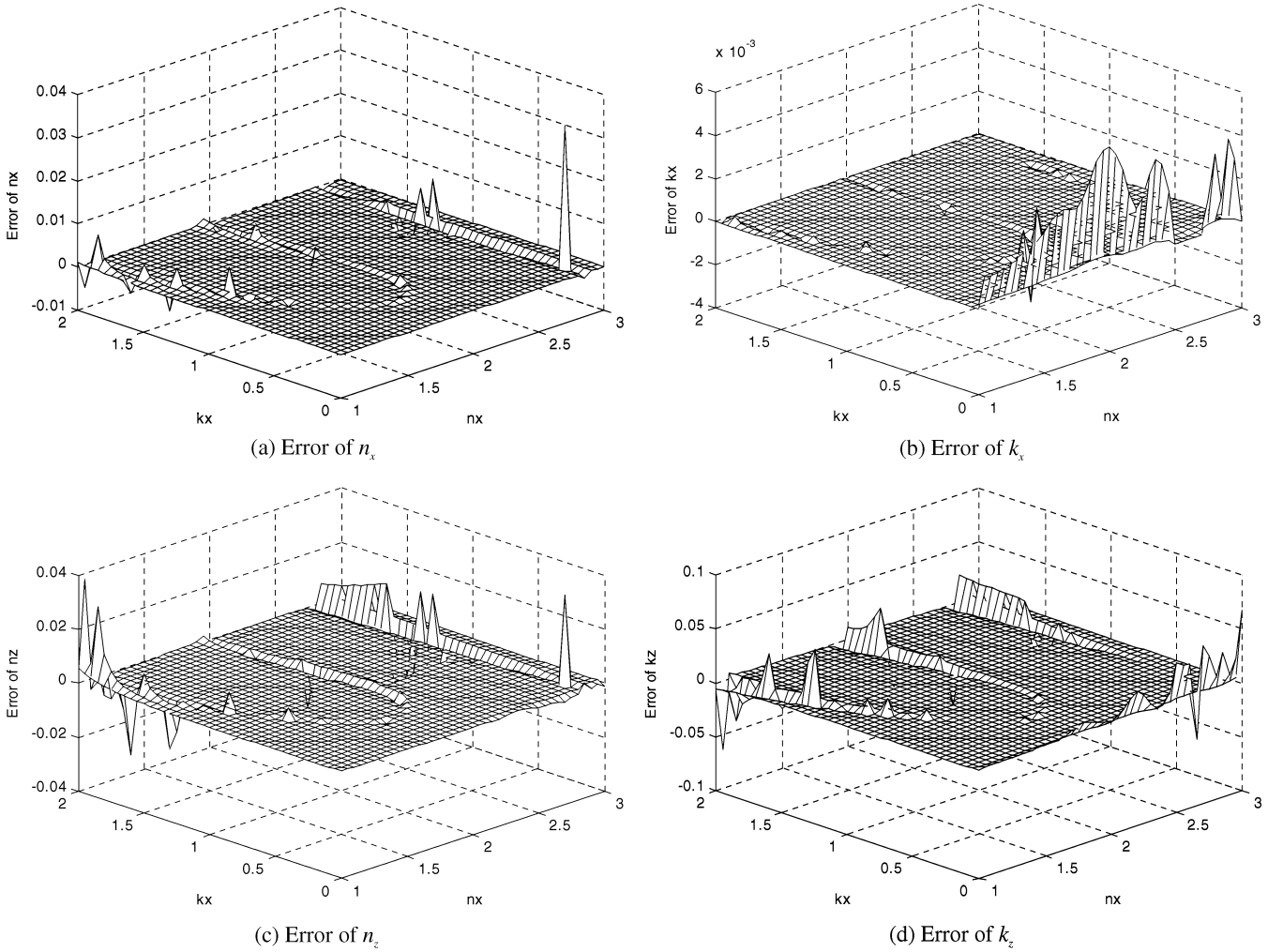

Figure 9. Influence of thickness variation ($\Delta t = 0.01$ μm) on calculation error of n and k (for three films: $t_1 = 3.0$ μm, $t_2 = 2.4$ μm, $t_3 = 1.8$ μm): (a) Error of n_x; (b) error of k_x; (c) error of n_z; (d) error of k_z.

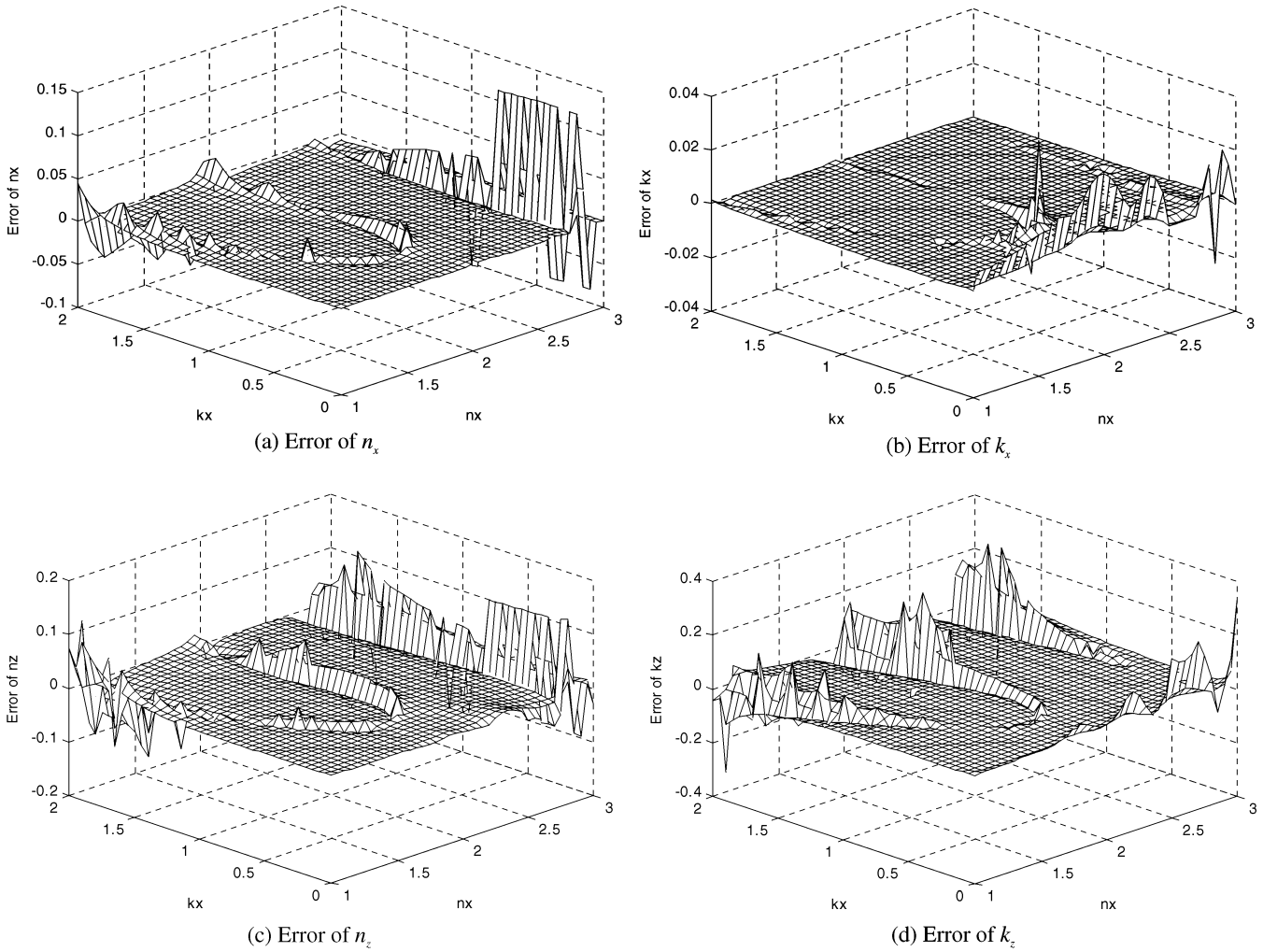

Figure 10. Influence of thickness variation ($\Delta t = 0.05$ μm) on calculation error of n and k (for three films: $t_1 = 3.0$ μm, $t_2 = 2.4$ μm, $t_3 = 1.8$ μm): (a) Error of n_x; (b) error of k_x; (c) error of n_z; (d) error of k_z.

45° incident angle in Table 1. However, the thickness values were extracted from the transmission spectra collected at 56° incident angle and there were minor differences between the thickness values used for 45° and 56° incident angle. The thickness values obtained for the 56° incident angle are indicated in parentheses in Table 1. Reference 16 presents a detailed discussion on the thickness differences. Figure 7 compares the resultant n and k spectra calculated from R/T ratios at 45° and 56° incident angles; in Figure 7, discontinuous points have been excluded. Clearly, the results at the two incident angles generally match well, although the results at 56° incident angle show more scattering, especially for the n_z and k_z spectra.

If the reflection and transmission spectra are error free, n and k can be extracted equally well from data collected at any incident angle between 0° and 90°. However, due to the existence of measurement error, accuracy of the resultant n and k will be dependent on the incident angle. Determination of the optimal incident angle for best n and k results is beyond the scope of this paper. In the following, we briefly discuss the influence of incident angle on n and k extraction. Generally speaking, for the same incident intensity, both the transmitted and reflected intensity will change as the incident angle changes. Since the incident intensity will always be the sum of transmitted intensity, reflected intensity and light absorption by the film, the transmitted intensity and the reflected intensity are expected to display a negative correlation for wavelength ranges where the absorption is not very strong. That is, when transmitted intensity increases, the reflected intensity will decrease, and vice visa. To reduce the error in R/T, neither R nor T should be too close to 0. Therefore, an optimal incident angle range may exist that provides a good signal/noise ratio for both R and T. For n_x and k_x, ideal incident angles will be those that provide a good signal/noise ratio for both R_s and T_s. The situation is more complicated for n_z and k_z since the achievement of good signal/noise ratio for both R_p and T_p is compromised by the need to limit the propagation of error of n_x and k_x on n_z and k_z. Rearranging eq 9 yields

$$n_z - ik_z = \frac{\sin\theta}{\sqrt{1 - \dfrac{\gamma_1^2(1)}{(\omega/c)^2}\dfrac{1}{(n_x - ik_x)^2}}} \tag{19}$$

Equation 19 indicates that the relative influence of $(n_x - ik_x)$ on n_z and k_z values is reduced if the magnitude of $\gamma_1(1)$ decreases. From eq 9, the magnitude of $\gamma_1(1)$ decreases with an increase of incident angle. The influence of errors in n_x and k_x on n_z and k_z values is minimized at grazing incidence ($\theta = 90°$). As a result, optimal incident angle for n_z and k_z should be the largest incident angle that provides satisfactory signal/noise ratio for both R_p and T_p.

5.3. Simulation Based on Previous Publications. Previous investigations have constructed n_x and k_x spectra for BPDA-PDA films based on an oscillator model and the Kramers−

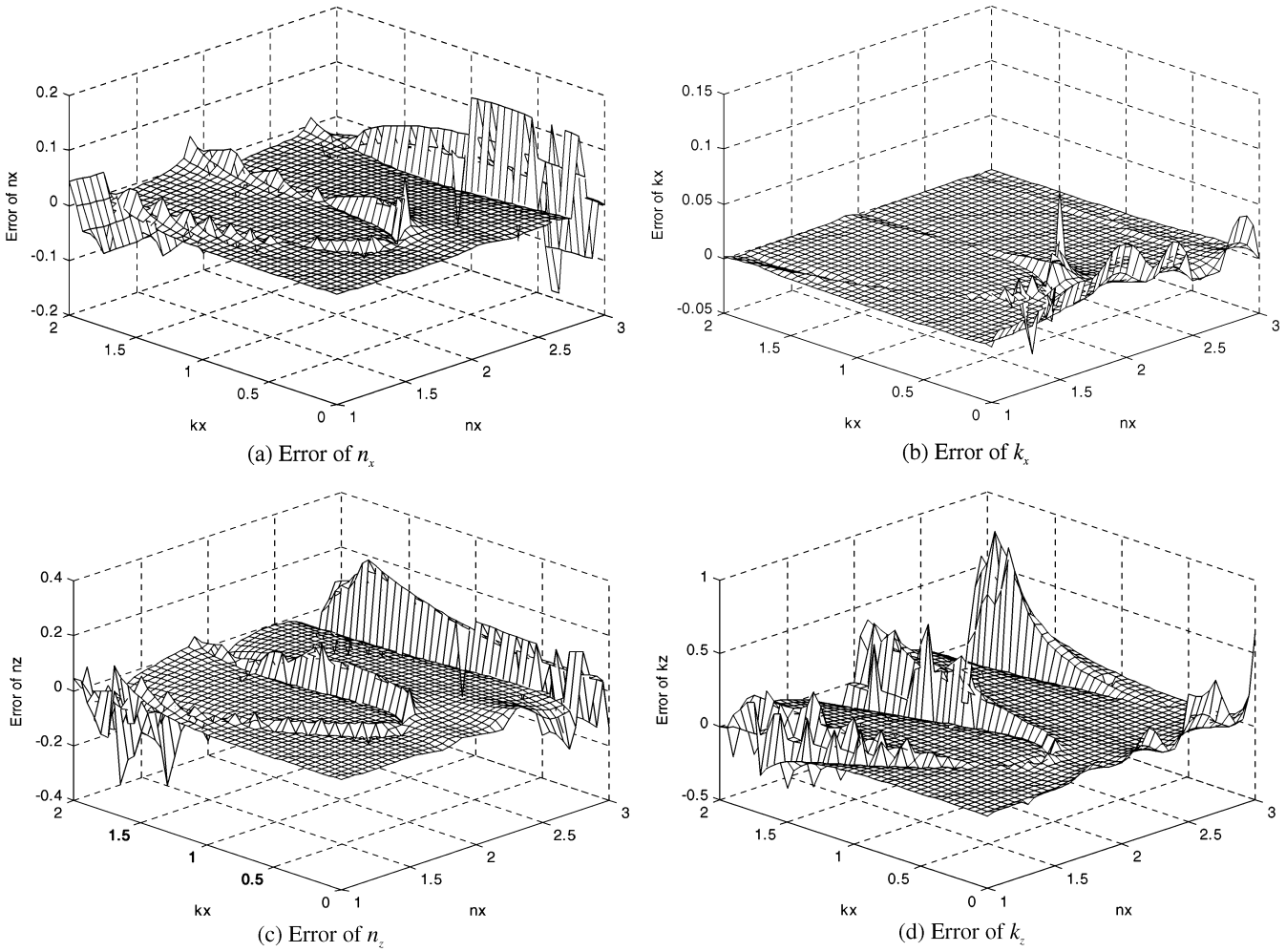

Figure 11. Influence of thickness variation ($\Delta t = 0.10$ μm) on calculation error of n and k (for three films: $t_1 = 3.0$ μm, $t_2 = 2.4$ μm, $t_3 = 1.8$ μm): (a) Error of n_x; (b) error of k_x; (c) error of n_z; (d) error of k_z.

Kronig relation.[18,19] We reconstructed the n_x and k_x spectra from a computer code kindly supplied by the authors of refs 18 and 19. Figure 8 compares the reconstructed n_x and k_x spectra with those reported in Figure 6. For this calculation, four vibrational modes (1774 cm^{-1} [ν_s(C═O), Imide I], 1717 cm^{-1} [ν_{as}(C═O), Imide I], 1516 cm^{-1} [C═C tangential stretch of PDA ring, C═C_{PDA}], and 1360 cm^{-1} [C−N−C axial str., Imide II]) and an isotropic term were considered.[18,19] The in-plane principle value of $n_x^{\infty} = 1.80$ is used based upon prism coupler measurement results at 1550 nm.[16] The measured n_x and k_x values match well with the values predicted by simulation. To the authors' knowledge, our studies are the first to report efforts to extract n_z and k_z values. Unfortunately, no literature values are currently available to verify the accuracy of n_z and k_z spectra.

5.4. Discussion on Influence of Variation in Film Thickness. In addition to experimental error on intensity measurements, sample nonuniformity and sample alignment also affect the accuracy of the calculated n and k values. Although uniform optical anisotropy has been established across the sample film, film thickness can vary significantly.[15,16] All of the above calculations are based on the average thickness across the sample area without considering the thickness variation. In addition, any misalignment between symmetric axes of the film and *XYZ* axes (Figure 1) will also result in error in the calculated n and k values. Since the BPDA-PDA films used in this study are isotropic in-plane, perfect alignment between the incident plane and X (or Y) axis is not required. However, if the sample surface is not perpendicular to the Z axis, the actual incident angle will differ from its preset value and this will result in an error in calculated n and k values. The following discussion will first address how to estimate the error due to neglect of thickness variation. Then a brief discussion on error caused by sample misalignment will be presented.

The thickness variation influences film transmittance and reflectance through a convolution with the nonuniformity in intensity of incident radiation. If we assume that the percentage of radiation intensity striking an area with thicknesses falling within the range $[t, t + \mathrm{d}t]$ can be represented by $f'(t)\,\mathrm{d}t$, then

$$\int_{t_{\min}}^{t_{\max}} f'(t)\,\mathrm{d}t = 1 \tag{20}$$

where $t_{\min}$ and $t_{\max}$ are the minimum and maximum thickness in the illuminated sample. $f'(t)$ is called the intensity weighted thickness distribution function.[16] For a total intensity (I) of radiation striking the sample, the transmittance after thickness variation correction ($T_{\Delta t}$) is

$$T_{\Delta t} = \frac{\int_{t_{\min}}^{t_{\max}} I\, f'(t)\, T(t)\,\mathrm{d}t}{I} = \int_{t_{\min}}^{t_{\max}} f'(t)\, T(t)\,\mathrm{d}t \tag{21}$$

where $T(t)$ is the transmittance if the sample has a uniform thickness t. Similarly, the reflectance after thickness variation

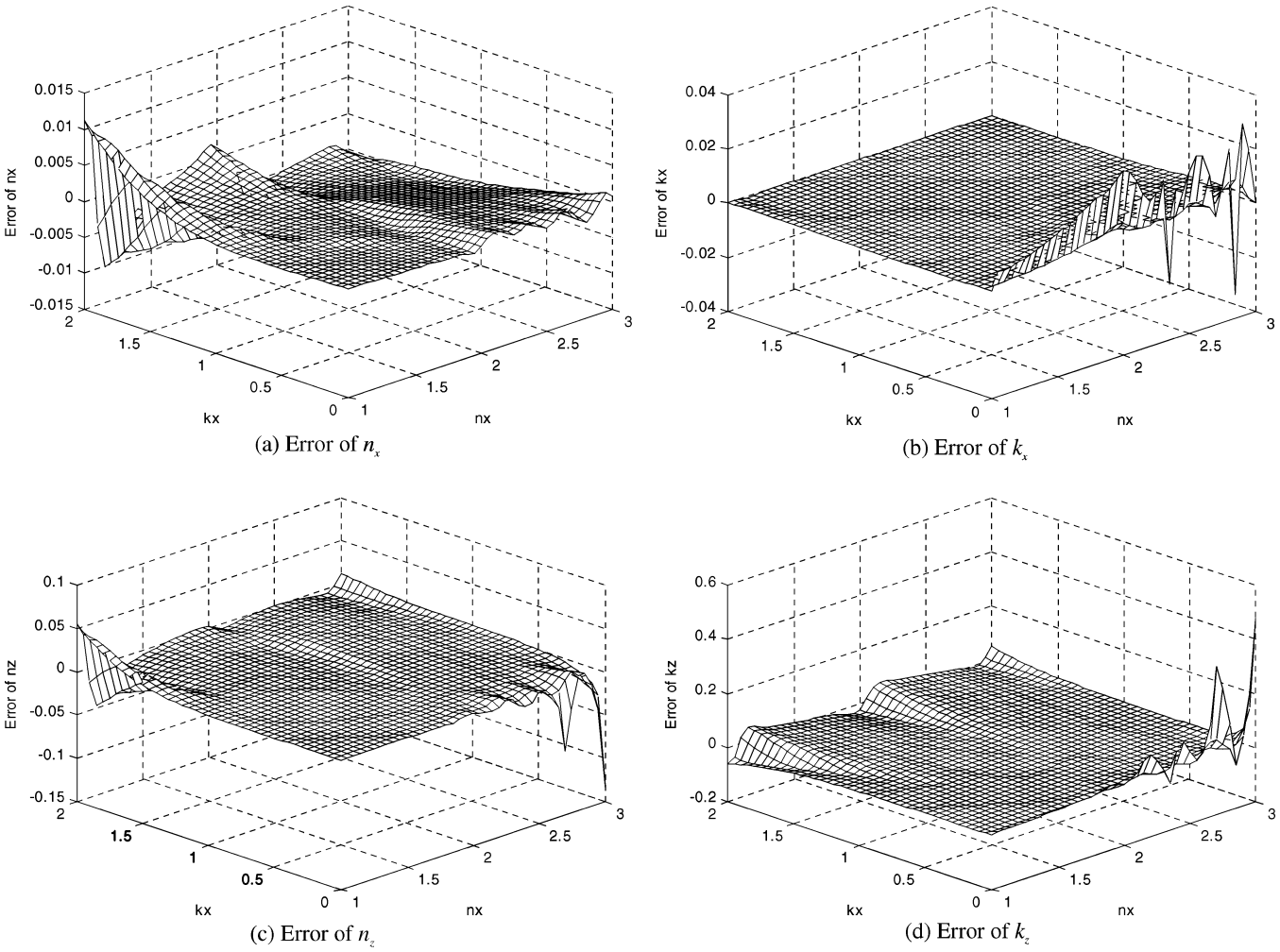

Figure 12. Influence of thickness variation ($\Delta t = 0.05$ μm) on calculation error of n and k (for five films: $t_1 = 3.0$ μm, $t_2 = 2.7$ μm, $t_3 = 2.4$ μm, $t_4 = 2.1$ μm, $t_5 = 1.8$ μm): (a) Error of n_x; (b) error of k_x; (c) error of n_z; (d) error of k_z.

correction ($R_{\Delta t}$) is

$$R_{\Delta t} = \int_{t_{\min}}^{t_{\max}} f'(t)\, R(t)\, \mathrm{d}t \tag{22}$$

Generally

$$\frac{R_{\Delta t}}{T_{\Delta t}} = \frac{\int_{t_{\min}}^{t_{\max}} f'(t)\, R(t)\, \mathrm{d}t}{\int_{t_{\min}}^{t_{\max}} f'(t)\, T(t)\, \mathrm{d}t} \neq \frac{R(\bar{t})}{T(\bar{t})} \tag{23}$$

where $\bar{t}$ is the intensity weighted average thickness.[16] If $R_{\Delta t}$ and $T_{\Delta t}$, which are transmittance and reflectance collected over an area with thickness variation, and $\bar{t}$, which is determined from the polarized transmission spectra in the transparent wavelength range,[16] are used to determine n and k, errors are inevitable as indicated by the inequality in eq 23. In the following, we present a brief discussion on how thickness variation across the sample film affects error in calculated n and k values and how such error can be reduced.

For simplification purpose, the sample film is assumed to be isotropic ($n_x = n_z$, $k_x = k_z$) and $f'(t)$ is assumed to follow uniform distribution

$$f'(t) = \frac{1}{2\Delta t} \tag{24}$$

where $\Delta t = (t_{\max} - t_{\min})/2$ is the intensity weighted half thickness span.[16] All simulations are for 1500 cm^{-1} and an incident angle of 45°. Given a certain pair of n_x and k_x, $R_{\Delta t}$ and $T_{\Delta t}$ of s- and p-polarized light of three films with intensities weighted average thicknesses of 3.0, 2.4, and 1.8 μm are calculated from eqs 21 and 22 by numerical integration. The intensity weighted half thickness span for the three films are assumed to be the same. Experimental error is not considered and $R_{\Delta t}$ and $T_{\Delta t}$ are used as input to extract n and k. The method described in the Data Analysis section is used to extract n_x, k_x, n_z, and k_z values. The thickness pairings are shown in Table 2a. In simulation, n_x is varied between 1 and 3 at a step size of 0.05, whereas k_x is varied between 0 and 2 at a step size of 0.05. The error in n or k is calculated by subtracting the true value from the extracted value. To expedite the computation, the "mesh-and-search" algorithm that was used for experimental data is not used. Instead, the Matlab function "fminsearch" is used in searching for optimal solutions because the given pair of n_x and k_x is expected to be a good initial guess in the absence of experimental error.

Figure 9a−d shows how errors of n_x, k_x, n_z, and k_z change over the square defined by [$1 \le n \le 3$, $0 \le k \le 2$] for $\Delta t = 0.01$ μm, respectively. Figures 10 and 11 show corresponding figures for $\Delta t = 0.05$ μm and $\Delta t = 0.10$ μm, respectively. It can be seen that the errors of n_z and k_z are larger than n_x and k_x, as expected. The propagation of error from n_x to n_z and k_z is obvious in some areas. The error of k is relatively larger if $k = 0$. This is due to the fact that, if a film is transparent and uniform

in thickness, the transmittance will approach 100% for some n at a specified wavelength and incident angle as a result of light interference. However, if thickness variation exists, transmittance will never reach 100%,[16] with an effect similar to absorption. This will result in positive error in calculated k values. When $k > 0$, the effect of decreased transmittance caused by thickness variations will be dwarfed by the absorption by the film so that the error in calculated k values will not be as significant as $k = 0$. For $\Delta t = 0.01$ μm, most of the calculated n and k values have errors below 0.01. Errors of n and k undergo substantial increase as Δt increases from 0.01 to 0.05 μm and to 0.10 μm. The n and k errors for $\Delta t = 0.05$ μm and $\Delta t = 0.10$ μm are >0.1 in many areas on the nk plane. Obviously, sample thickness variation is critical in determining the accuracy of calculated n and k values.

In the Data Analysis section, to reduce the influence of experimental error, we proposed the use of five films with difference thicknesses (four R/T ratios). Using five films, as compared to three films, also reduces the influence of thickness variation on the errors in calculated n and k values. A similar simulation study to that described above has been performed. Five films with intensity weighted average thicknesses of 3.0, 2.7, 2.4, 2.1, and 1.8 μm are used. For all five films, $\Delta t = 0.05$. The thickness pairings are shown in Table 2b and the simulation results are shown in Figure 12. Compared to Figure 10, the errors in Figure 12 for both n and k values are significantly smaller. Except for regions where k is close to 0 or n is close to 1, errors for n_x, k_x, and n_z are smaller than 0.01, whereas the error in k_z is smaller than 0.05. Therefore, if sample thickness variation is large, more films with different thicknesses should be used in order to improve the accuracy of calculated n and k values.

The error caused by sample misalignment can be estimated in a similar way and will only be briefly discussed. If the difference between the actual incident angle and the preset value (θ) due to misalignment is $\Delta\theta$, the measured R/T ratios will satisfy the following equation:

$$\frac{(R_p/T_p)_{t=t_1}}{(R_p/T_p)_{t=t_2}}\Big|_{\text{measured}} = \frac{|\exp[i\gamma_{1,\theta+\Delta\theta}(1)t_1] - \exp[-i\gamma_{1,\theta+\Delta\theta}(1)t_1]|^2}{|\exp[i\gamma_{1,\theta+\Delta\theta}(1)t_2] - \exp[-i\gamma_{1,\theta+\Delta\theta}(1)t_2]|^2} \quad (25)$$

and

$$\frac{(R_s/T_s)_{t=t_1}}{(R_s/T_s)_{t=t_2}}\Big|_{\text{measured}} = \frac{|\exp[i\gamma_{3,\theta+\Delta\theta}(1)t_1] - \exp[-i\gamma_{3,\theta+\Delta\theta}(1)t_1]|^2}{|\exp[i\gamma_{3,\theta+\Delta\theta}(1)t_2] - \exp[-i\gamma_{3,\theta+\Delta\theta}(1)t_2]|^2} \quad (26)$$

where $\gamma_{1,\theta+\Delta\theta}(1)$ and $\gamma_{3,\theta+\Delta\theta}(1)$ are calculated by replacing θ with $\theta + \Delta\theta$ in eqs 9 and 13. For a film with n and k at a particular wavelength, the error of extracted n and k values for a specific $\Delta\theta$ can be estimated by substituting eq 25 or eq 26 into eq 18 to calculate the target function $g(n,k)$ and then searching for optimal n and k values and comparing optimal values with the actual ones.

6. Conclusions

A new method has been proposed to extract complex refractive indices ($n - ik$) of films with biaxial symmetry from polarized transmission and reflection spectra. The method is based on a simple relationship between complex refractive indices and the reflectance/transmittance ratio (R/T ratio) of two films of different thicknesses but with the same optical anisotropy. With known thickness values, anisotropic n and k spectra within a particular wavelength range can be extracted from s- and p-polarized R/T ratios at oblique incidence. Using R/T ratios in calculation reduces errors caused by light scattering due to sample surface roughness. It also precludes the necessity for an accurate reflection background. No a priori assumptions on the relationship among n, k, and wavelength are required. Although the method is developed for anisotropic films, it can be readily applied to isotropic films to extract n and k spectra without assuming a specific relationship among n, k, and wavelength. As a demonstration, the R/T ratio method is used to extract the anisotropic complex refractive indices of BPDA-PDA films in the infrared range. The resultant n and k spectra compare well with simulations based on known n and k values. The accuracy of n and k spectra is affected mostly by experimental error in reflection and transmission spectra collection, thickness variation across the sample film, and sample alignment.

Acknowledgment. The authors thank Mr. Joshua Stapleton and Professor David Allara for kindly supplying FORTRAN codes on infrared spectral simulation and Dr. Weontae Oh and Professor Sankar Nair for access to the infrared spectrometer. We also thank Applied Materials for a fellowship for Jie Diao.

Appendix I. Derivation of Transmittance and Reflectance Expression for Polarized Light Passing through a Freestanding Film

The starting point for the derivation is the following equation, which describes the propagation of electromagnetic waves in a medium with a dielectric tensor of ϵ and permeability of μ:[10]

$$\mathbf{k} \times (\mathbf{k} \times \mathbf{E}) + \omega^2\mu\epsilon\mathbf{E} = 0 \quad (27)$$

where $\mathbf{E}$ is the electric field vector, $\mathbf{k}$ the wave vector, $\mathbf{k} = (\omega/c)n\mathbf{s}$, with $\mathbf{s}$ as a unit vector in the direction of propagation, ω the frequency, and c the speed of light in a vacuum. The dielectric tensor ϵ can be written in matrix form as

$$\epsilon = \begin{pmatrix} \epsilon_{xx} & \epsilon_{xy} & \epsilon_{xz} \\ \epsilon_{yx} & \epsilon_{yy} & \epsilon_{yz} \\ \epsilon_{zx} & \epsilon_{zy} & \epsilon_{zz} \end{pmatrix} \quad (28)$$

The wave vector $\mathbf{k}$ can be described in terms of X, Y, and Z components (α, β, and γ): $\mathbf{k} = \alpha\mathbf{x} + \beta\mathbf{y} + \gamma\mathbf{z}$. The electric field of the plane electromagnetic waves can be written as

$$\mathbf{E} = \sum_{\sigma=1}^{4} A_\sigma \mathbf{p}_\sigma \exp[i(\varpi t - \alpha x - \beta y - \gamma_\sigma z)] \quad (29)$$

where A_σ and $\mathbf{p}_\sigma$ are the amplitude of the electric field and the unit vector in the same direction as the electric field corresponding to γ_σ, respectively. The magnetic filed vector H can be expressed in a similar manner

$$\mathbf{H} = \sum_{\sigma=1}^{4} A_\sigma \mathbf{q}_\sigma \exp[i(\varpi t - \alpha x - \beta y - \gamma_\sigma z)] \quad (30)$$

where $\mathbf{q}_\sigma$ is the unit vector in the same direction as the magnetic field corresponding to γ_σ. $\mathbf{p}_\sigma$ and $\mathbf{q}_\sigma$ are perpendicular to each

other and are related by eq 31

$$\mathbf{q}_\sigma(n) = \frac{c\mathbf{k}_\sigma(n)}{\omega\mu} \times \mathbf{p}_\sigma(n) \tag{31}$$

The following relationship between electric fields in adjacent layers can be obtained by solving electromagnetic boundary value equations:[9,10]

$$\begin{pmatrix} A_1(n-1) \\ A_2(n-1) \\ A_3(n-1) \\ A_4(n-1) \end{pmatrix} = \mathbf{D}^{-1}(n-1)\mathbf{D}(n)\mathbf{P}(n) \begin{pmatrix} A_1(n) \\ A_2(n) \\ A_3(n) \\ A_4(n) \end{pmatrix} \tag{32}$$

where matrices

$$\mathbf{D}(n) = \begin{pmatrix} \mathbf{x}\cdot\mathbf{p}_1(n) & \mathbf{x}\cdot\mathbf{p}_2(n) & \mathbf{x}\cdot\mathbf{p}_3(n) & \mathbf{x}\cdot\mathbf{p}_4(n) \\ \mathbf{y}\cdot\mathbf{q}_1(n) & \mathbf{y}\cdot\mathbf{q}_2(n) & \mathbf{y}\cdot\mathbf{q}_3(n) & \mathbf{y}\cdot\mathbf{q}_4(n) \\ \mathbf{y}\cdot\mathbf{p}_1(n) & \mathbf{y}\cdot\mathbf{p}_2(n) & \mathbf{y}\cdot\mathbf{p}_3(n) & \mathbf{y}\cdot\mathbf{p}_4(n) \\ \mathbf{x}\cdot\mathbf{q}_1(n) & \mathbf{x}\cdot\mathbf{q}_2(n) & \mathbf{x}\cdot\mathbf{q}_3(n) & \mathbf{x}\cdot\mathbf{q}_4(n) \end{pmatrix} \tag{33}$$

and

$$\mathbf{P}(n) = \begin{pmatrix} \exp[i\gamma_1(n)t(n)] & 0 & 0 & 0 \\ 0 & \exp[i\gamma_2(n)t(n)] & 0 & 0 \\ 0 & 0 & \exp[i\gamma_3(n)t(n)] & 0 \\ 0 & 0 & 0 & \exp[i\gamma_4(n)t(n)] \end{pmatrix} \tag{34}$$

are called dynamical matrix and propagation matrix, respectively.

Because all layers are stacked in the Z direction and each layer is assumed to be homogeneous in the XY plane, α and β will remain constant throughout the layered media. Therefore, the two components (α, β) of the propagation vector are chosen as the dynamical variables characterizing the electromagnetic waves propagating in the layered media. Given α and β, the z component γ is determined directly from eq 27, or equivalently

$$\begin{pmatrix} \omega^2\mu\epsilon_{xx} - \beta^2 - \gamma^2 & \omega^2\mu\epsilon_{xy} + \alpha\beta & \omega^2\mu\epsilon_{xz} + \alpha\gamma \\ \omega^2\mu\epsilon_{yx} + \alpha\beta & \omega^2\mu\epsilon_{yy} - \alpha^2 - \gamma^2 & \omega^2\mu\epsilon_{yz} + \beta\gamma \\ \omega^2\mu\epsilon_{zx} + \alpha\gamma & \omega^2\mu\epsilon_{zy} + \beta\gamma & \omega^2\mu\epsilon_{zz} - \alpha^2 - \beta^2 \end{pmatrix} \times \begin{pmatrix} E_x \\ E_y \\ E_z \end{pmatrix} = 0 \tag{35}$$

To have a nontrivial plane-wave solution, the determinant of the matrix in eq 35 must vanish, that is

$$\det\begin{pmatrix} \omega^2\mu\epsilon_{xx} - \beta^2 - \gamma^2 & \omega^2\mu\epsilon_{xy} + \alpha\beta & \omega^2\mu\epsilon_{xz} + \alpha\gamma \\ \omega^2\mu\epsilon_{yx} + \alpha\beta & \omega^2\mu\epsilon_{yy} - \alpha^2 - \gamma^2 & \omega^2\mu\epsilon_{yz} + \beta\gamma \\ \omega^2\mu\epsilon_{zx} + \alpha\gamma & \omega^2\mu\epsilon_{zy} + \beta\gamma & \omega^2\mu\epsilon_{zz} - \alpha^2 - \beta^2 \end{pmatrix} = 0 \tag{36}$$

For a biaxial absorbing medium with the symmetry axes coinciding with X, Y, and Z axes, the dielectric tensor can be written as

$$\epsilon = \begin{pmatrix} \omega^2\mu\epsilon_0(n_x - ik_x)^2 & 0 & 0 \\ 0 & \omega^2\mu\epsilon_0(n_y - ik_y)^2 & 0 \\ 0 & 0 & \omega^2\mu\epsilon_0(n_z - ik_z)^2 \end{pmatrix} \tag{37}$$

If the light is incident from vacuum (or air) in the XZ plane with an incident angle of θ (Figure 1a), then $\alpha = (\omega/c)\sin\theta, \beta = 0$. Substitution of eq 37 into eq 36 leads to

$$\det\begin{pmatrix} (\omega/c)^2(n_x - ik_x)^2 - \gamma^2 & 0 & \alpha\gamma \\ 0 & (\omega/c)^2(n_y - ik_y)^2 - \alpha^2 - \gamma^2 & 0 \\ \alpha\gamma & 0 & (\omega/c)^2(n_z - ik_z)^2 - \alpha^2 \end{pmatrix} = 0 \tag{38}$$

In deriving eq 38, the relation $c = 1/(\mu\epsilon_0)^{1/2}$ is used. The solutions to eq 38 are

$$\gamma_{1,2} = \pm\sqrt{(\omega/c)^2(n_x - ik_x)^2 - \frac{(n_x - ik_x)^2}{(n_z - ik_z)^2}\alpha^2} \tag{39}$$

$$\gamma_{3,4} = \pm\sqrt{(\omega/c)^2(n_y - ik_y)^2 - \alpha^2} \tag{40}$$

In the following discussion, we specify γ_1 and γ_3 as the two roots with positive real parts; these two roots correspond to the two partial waves propagating in the positive Z direction. For γ_1, substitution of eq 39 into eq 38 yields

$$\begin{pmatrix} (\omega/c)^2(n_x - ik_x)^2 - \gamma_1^2 & 0 & \alpha\gamma_1 \\ 0 & (\omega/c)^2(n_y - ik_y)^2 - \alpha^2 - (\omega/c)^2(n_x - ik_x)^2 + \dfrac{(n_x - ik_x)^2}{(n_z - ik_z)^2}\alpha^2 & 0 \\ \alpha\gamma_1 & 0 & (\omega/c)^2(n_z - ik_z)^2 - \alpha^2 \end{pmatrix}\begin{pmatrix} E_x \\ E_y \\ E_z \end{pmatrix} = 0 \tag{41}$$

If

$$\alpha^2\frac{(n_z - ik_z)^2 - (n_x - ik_x)^2}{(\omega/c)^2(n_z - ik_z)^2} \neq (n_y - ik_y)^2 - (n_x - ik_x)^2 \tag{42}$$

it can be concluded from eq 41 that

$$E_y = 0 \qquad \frac{E_x}{E_z} = \frac{-(\omega/c)^2(n_z - ik_z)^2 + \alpha^2}{\alpha\gamma_1} \tag{43}$$

It is worth pointing out that rearranging eq 39 leads to

$$\frac{(\omega/c)^2(n_z - ik_z)^2 - \alpha^2}{\alpha\gamma_1} = \frac{\alpha\gamma_1}{(\omega/c)^2(n_x - ik_x)^2 - \gamma_1^2} \tag{44}$$

Thus we can define $\mathbf{p}_1'$ and unit vector $\mathbf{p}_1$ as

$$\mathbf{p}_1' = (-(\omega/c)^2(n_z - ik_z)^2 + \alpha^2 \;\; 0 \;\; \alpha\gamma_1)^T \tag{45}$$

$$\mathbf{p}_1 = \frac{\mathbf{p}_1'}{|\mathbf{p}_1'|} = \begin{pmatrix} \dfrac{-(\omega/c)^2(n_z - ik_z)^2 + \alpha^2}{|\mathbf{p}_1'|} & 0 & \dfrac{\alpha\gamma_1}{|\mathbf{p}_1'|} \end{pmatrix}^T = \begin{pmatrix} p_{11} \\ 0 \\ p_{13} \end{pmatrix} \tag{46}$$

where

$$p_{11} = \frac{-(\omega/c)^2(n_z - ik_z)^2 + \alpha^2}{|\mathbf{p}_1'|} \qquad p_{13} = \frac{\alpha\gamma_1}{|\mathbf{p}_1'|} \tag{47}$$

Subsequently

$$\mathbf{q}_1 = \frac{c}{\omega\mu}\mathbf{k}_1 \times \mathbf{p}_1 = \frac{c}{\omega\mu}\begin{pmatrix} \alpha \\ 0 \\ \gamma_1 \end{pmatrix} \times \begin{pmatrix} p_{11} \\ 0 \\ p_{13} \end{pmatrix} = \begin{pmatrix} 0 \\ \dfrac{c}{\omega\mu}(\gamma_1 \cdot p_{11} - \alpha \cdot p_{13}) \\ 0 \end{pmatrix} \tag{48}$$

Similarly, for $\gamma_2 = -\gamma_1$, we have

$$\mathbf{p}_2' = (-(\omega/c)^2(n_z - ik_z)^2 + \alpha^2 \; 0 \; -\alpha\gamma_1)^T \tag{49}$$

$$\mathbf{p}_2 = \frac{\mathbf{p}_2'}{|\mathbf{p}_2'|} = \begin{pmatrix} \dfrac{-(\omega/c)^2(n_z - ik_z)^2 + \alpha^2}{|\mathbf{p}_2'|} & 0 & \dfrac{-\alpha\gamma_1}{|\mathbf{p}_2'|} \end{pmatrix}^T = \begin{pmatrix} p_{21} \\ 0 \\ p_{23} \end{pmatrix} \tag{50}$$

where

$$p_{21} = \frac{-(\omega/c)^2(n_z - ik_z)^2 + \alpha^2}{|\mathbf{p}_2'|} \qquad p_{23} = \frac{-\alpha\gamma_1}{|\mathbf{p}_2'|} \tag{51}$$

and

$$\mathbf{q}_2 = \frac{c}{\omega\mu}\mathbf{k}_2 \times \mathbf{p}_2 = \frac{c}{\omega\mu}\begin{pmatrix}\alpha\\0\\-\gamma_1\end{pmatrix} \times \begin{pmatrix}p_{21}\\0\\p_{23}\end{pmatrix} = \begin{pmatrix}0\\\frac{c}{\omega\mu}(-\gamma_1 \cdot p_{21} - \alpha \cdot p_{23})\\0\end{pmatrix} \tag{52}$$

In the above expressions: $|\mathbf{p}_1'| = |\mathbf{p}_2'|$, $p_{11} = p_{21}$ and $p_{13} = -p_{23}$.

For γ_3, substitution of eq 40 into eq 38 yields

$$\begin{pmatrix}(\omega/c)^2(n_x - ik_x)^2 - {\gamma_3}^2 & 0 & \alpha\gamma_3\\0 & 0 & 0\\\alpha\gamma_3 & 0 & (\omega/c)^2(n_z - ik_z)^2 - \alpha^2\end{pmatrix}\begin{pmatrix}E_x\\E_y\\E_z\end{pmatrix} = 0 \tag{53}$$

From eq 53

$$\begin{pmatrix}(\omega/c)^2(n_x - ik_x)^2 - {\gamma_3}^2 & \alpha\gamma_3\\\alpha\gamma_3 & (\omega/c)^2(n_z - ik_z)^2 - \alpha^2\end{pmatrix}\begin{pmatrix}E_x\\E_z\end{pmatrix} = 0 \tag{54}$$

The inequality in eq 42 is equivalent to

$$\det\begin{pmatrix}(\omega/c)^2(n_x - ik_x)^2 - {\gamma_3}^2 & \alpha\gamma_3\\\alpha\gamma_3 & (\omega/c)^2(n_z - ik_z)^2 - \alpha^2\end{pmatrix} \neq 0 \tag{55}$$

which implies that

$$E_x = E_z = 0 \tag{56}$$

Thus, we can choose $\mathbf{p}_3$ as

$$\mathbf{p}_3 = \begin{pmatrix}0\\1\\0\end{pmatrix} \tag{57}$$

Therefore

$$\mathbf{q}_3 = \frac{c}{\omega\mu}\mathbf{k}_3 \times \mathbf{p}_3 = \frac{c}{\omega\mu}\begin{pmatrix}\alpha\\0\\\gamma_3\end{pmatrix} \times \begin{pmatrix}0\\1\\0\end{pmatrix} = \begin{pmatrix}-\frac{c}{\omega\mu}\gamma_3\\0\\\frac{c}{\omega\mu}\alpha\end{pmatrix} \tag{58}$$

Similarly, for $\gamma_4 = -\gamma_3$, we have

$$\mathbf{p}_4 = \begin{pmatrix}0\\1\\0\end{pmatrix} \tag{59}$$

and

$$\mathbf{q}_4 = \frac{c}{\omega\mu}\mathbf{k}_4 \times \mathbf{p}_4 = \frac{c}{\omega\mu}\begin{pmatrix}\alpha\\0\\-\gamma_3\end{pmatrix} \times \begin{pmatrix}0\\1\\0\end{pmatrix} = \begin{pmatrix}\frac{c}{\omega\mu}\gamma_3\\0\\\frac{c}{\omega\mu}\alpha\end{pmatrix} \tag{60}$$

In deriving $\mathbf{p}_1 - \mathbf{p}_4$, the inequality expressed in eq 42 is assumed. However, it is easy to verify that the expressions for $\mathbf{p}_1 - \mathbf{p}_4$ are still valid even if

$$\alpha^2\frac{(n_z - ik_z)^2 - (n_x - ik_x)^2}{(\omega/c)^2(n_z - ik_z)^2} = (n_y - ik_y)^2 - (n_x - ik_x)^2 \tag{61}$$

Thus

$$\begin{aligned}\mathbf{D} &= \begin{pmatrix} \mathbf{x}\cdot\mathbf{p}_1 & \mathbf{x}\cdot\mathbf{p}_2 & \mathbf{x}\cdot\mathbf{p}_3 & \mathbf{x}\cdot\mathbf{p}_4 \\ \mathbf{y}\cdot\mathbf{q}_1 & \mathbf{y}\cdot\mathbf{q}_2 & \mathbf{y}\cdot\mathbf{q}_3 & \mathbf{y}\cdot\mathbf{q}_4 \\ \mathbf{y}\cdot\mathbf{p}_1 & \mathbf{y}\cdot\mathbf{p}_2 & \mathbf{y}\cdot\mathbf{p}_3 & \mathbf{y}\cdot\mathbf{p}_4 \\ \mathbf{x}\cdot\mathbf{q}_1 & \mathbf{x}\cdot\mathbf{q}_2 & \mathbf{x}\cdot\mathbf{q}_3 & \mathbf{x}\cdot\mathbf{q}_4 \end{pmatrix} \\ &= \begin{pmatrix} p_{11} & p_{21} & 0 & 0 \\ \frac{c}{\omega\mu}(\gamma_1\cdot p_{11} - \alpha\cdot p_{13}) & \frac{c}{\omega\mu}(-\gamma_1\cdot p_{21} - \alpha\cdot p_{23}) & 0 & 0 \\ 0 & 0 & 1 & 1 \\ 0 & 0 & -\frac{c}{\omega\mu}\gamma_3 & \frac{c}{\omega\mu}\gamma_3 \end{pmatrix} \\ &= \begin{pmatrix} \mathbf{D}_{UL} & \mathbf{O} \\ \mathbf{O} & \mathbf{D}_{LR} \end{pmatrix}\end{aligned} \tag{62}$$

where

$$\mathbf{D}_{\mathrm{UL}} = \begin{pmatrix} p_{11} & p_{21} \\ \frac{c}{\omega\mu}(\gamma_1\cdot p_{11} - \alpha\cdot p_{13}) & \frac{c}{\omega\mu}(-\gamma_1\cdot p_{21} - \alpha\cdot p_{23}) \end{pmatrix} \tag{63}$$

$$\mathbf{D}_{\mathrm{LR}} = \begin{bmatrix} 1 & 1 \\ -\frac{c}{\omega\mu}\gamma_3 & \frac{c}{\omega\mu}\gamma_3 \end{bmatrix} \tag{64}$$

$$\mathbf{O} = \begin{pmatrix} 0 & 0 \\ 0 & 0 \end{pmatrix} \tag{65}$$

and

$$\begin{aligned}\mathbf{P} &= \begin{pmatrix} \exp[i\gamma_1 t] & 0 & 0 & 0 \\ 0 & \exp[-i\gamma_1 t] & 0 & 0 \\ 0 & 0 & \exp[i\gamma_3 t] & 0 \\ 0 & 0 & 0 & \exp[-i\gamma_3 t] \end{pmatrix} \\ &= \begin{pmatrix} \mathbf{P}_{\mathrm{UL}} & \mathbf{O} \\ \mathbf{O} & \mathbf{P}_{\mathrm{LR}} \end{pmatrix}\end{aligned} \tag{66}$$

where

$$\mathbf{P}_{\mathrm{UL}} = \begin{pmatrix} \exp[i\gamma_1 t] & 0 \\ 0 & \exp[-i\gamma_1 t] \end{pmatrix} \tag{67}$$

$$\mathbf{P}_{\mathrm{LR}} = \begin{pmatrix} \exp[i\gamma_3 t] & 0 \\ 0 & \exp[-i\gamma_3 t] \end{pmatrix} \tag{68}$$

In the above expressions, subscripts UL and LR are used to denote "upper left" and "lower right", respectively. The inverse of **D** is

$$\mathbf{D}^{-1} = \begin{pmatrix} \mathbf{D}_{\mathrm{UL}}{}^{-1} & \mathbf{O} \\ \mathbf{O} & \mathbf{D}_{\mathrm{LR}}{}^{-1} \end{pmatrix} \tag{69}$$

For a layered structure of air(0)−film(1)−air(2)

$$\begin{pmatrix} A_1(0) \\ A_2(0) \\ A_3(0) \\ A_4(0) \end{pmatrix} = \mathbf{M}\begin{pmatrix} A_1(2) \\ A_2(2) \\ A_3(2) \\ A_4(2) \end{pmatrix} = \mathbf{D}^{-1}(0)\mathbf{D}(1)\mathbf{P}(1)\mathbf{D}^{-1}(1)\mathbf{D}(2)\begin{pmatrix} A_1(2) \\ A_2(2) \\ A_3(2) \\ A_4(2) \end{pmatrix} \tag{70}$$

Because phase 0 and phase 2 are both air

$$\mathbf{D}(0) = \mathbf{D}(2) \tag{71}$$

Also, because phase 2 is the last layer, there are no backward waves

$$A_2(2) = A_2(4) = 0 \tag{72}$$

Now eq 70 can be written as

$$\begin{aligned}
\begin{pmatrix} A_1(0) \\ A_2(0) \\ A_3(0) \\ A_4(0) \end{pmatrix} &= \mathbf{D}^{-1}(0)\mathbf{D}(1)\mathbf{P}(1)\mathbf{D}^{-1}(1)\mathbf{D}(0)\begin{pmatrix} A_1(2) \\ 0 \\ A_3(2) \\ 0 \end{pmatrix} \\
&= \begin{pmatrix} \mathbf{D}_{\mathrm{UL}}{}^{-1}(0) & \mathbf{O} \\ \mathbf{O} & \mathbf{D}_{\mathrm{LR}}{}^{-1}(0) \end{pmatrix}\begin{pmatrix} \mathbf{D}_{\mathrm{UL}}(1) & \mathbf{O} \\ \mathbf{O} & \mathbf{D}_{\mathrm{LR}}(1) \end{pmatrix}\begin{pmatrix} \mathbf{P}_{\mathrm{UL}}(1) & \mathbf{O} \\ \mathbf{O} & \mathbf{P}_{\mathrm{LR}}(1) \end{pmatrix}\begin{pmatrix} \mathbf{D}_{\mathrm{UL}}{}^{-1}(1) & \mathbf{O} \\ \mathbf{O} & \mathbf{D}_{\mathrm{LR}}{}^{-1}(1) \end{pmatrix}\begin{pmatrix} \mathbf{D}_{\mathrm{UL}}(0) & \mathbf{O} \\ \mathbf{O} & \mathbf{D}_{\mathrm{LR}}(0) \end{pmatrix}\begin{pmatrix} A_1(2) \\ 0 \\ A_3(2) \\ 0 \end{pmatrix} \\
&= \begin{pmatrix} \mathbf{D}_{\mathrm{UL}}{}^{-1}(0)\mathbf{D}_{\mathrm{UL}}(1)\mathbf{P}_{\mathrm{UL}}(1)\mathbf{D}_{\mathrm{UL}}{}^{-1}(1)\mathbf{D}_{\mathrm{UL}}(0) & \mathbf{O} \\ \mathbf{O} & \mathbf{D}_{\mathrm{LR}}{}^{-1}(0)\mathbf{D}_{\mathrm{LR}}(1)\mathbf{P}_{\mathrm{LR}}(1)\mathbf{D}_{\mathrm{LR}}{}^{-1}(1)\mathbf{D}_{\mathrm{LR}}(0) \end{pmatrix}\begin{pmatrix} A_1(2) \\ 0 \\ A_3(2) \\ 0 \end{pmatrix}
\end{aligned} \tag{73}$$

Equation 73 can be written as two separate equations

$$\begin{pmatrix} A_1(0) \\ A_2(0) \end{pmatrix} = \mathbf{D}_{\mathrm{UL}}{}^{-1}(0)\mathbf{D}_{\mathrm{UL}}(1)\mathbf{P}_{\mathrm{UL}}(1)\mathbf{D}_{\mathrm{UL}}{}^{-1}(1)\mathbf{D}_{\mathrm{UL}}(0)\begin{pmatrix} A_1(2) \\ 0 \end{pmatrix} \tag{74}$$

and

$$\begin{pmatrix} A_3(0) \\ A_4(0) \end{pmatrix} = \mathbf{D}_{\mathrm{LR}}{}^{-1}(0)\mathbf{D}_{\mathrm{LR}}(1)\mathbf{P}_{\mathrm{LR}}(1)\mathbf{D}_{\mathrm{LR}}{}^{-1}(1)\mathbf{D}_{\mathrm{LR}}(0)\begin{pmatrix} A_3(2) \\ 0 \end{pmatrix} \tag{75}$$

Because $\gamma_{1,2}$ and $\gamma_{3,4}$ correspond to p- and s-polarized light, respectively, eqs 74 and 75 can be used to calculate the transmittance and reflectance of p- and s-polarized light, respectively. Here we start with s-polarized light. For propagation in air

$$\gamma_3(0) = (\omega/c)\sqrt{n_0{}^2 - \sin^2\theta} \tag{76}$$

Thus

$$\mathbf{D}_{\mathrm{LR}}(0) = \begin{pmatrix} 1 & 1 \\ -\frac{1}{\mu}\sqrt{n_0{}^2 - \sin^2\theta} & \frac{1}{\mu}\sqrt{n_0{}^2 - \sin^2\theta} \end{pmatrix} \tag{77}$$

$$\mathbf{D}_{\mathrm{LR}}{}^{-1}(0) = \begin{pmatrix} 1/2 & -\dfrac{\mu}{2\sqrt{n_0{}^2 - \sin^2\theta}} \\ 1/2 & \dfrac{\mu}{2\sqrt{n_0{}^2 - \sin^2\theta}} \end{pmatrix} \tag{78}$$

For propagation in the film

$$\gamma_3(1) = (\omega/c)\sqrt{(n_y - ik_y)^2 - \sin^2\theta} \tag{79}$$

Thus

$$\mathbf{D}_{\mathrm{LR}}(1) = \begin{pmatrix} 1 & 1 \\ -\frac{1}{\mu}\sqrt{(n_y - ik_y)^2 - \sin^2\theta} & \frac{1}{\mu}\sqrt{(n_y - ik_y)^2 - \sin^2\theta} \end{pmatrix} \tag{80}$$

$$\mathbf{D}_{\mathrm{LR}}^{-1}(1) = \begin{pmatrix} 1/2 & -\dfrac{\mu}{2\sqrt{(n_y - ik_y)^2 - \sin^2\theta}} \\ 1/2 & \dfrac{\mu}{2\sqrt{(n_y - ik_y)^2 - \sin^2\theta}} \end{pmatrix} \tag{81}$$

$$\mathbf{P}_{\mathrm{LR}}(1) = \begin{pmatrix} \exp[i\gamma_3(1)t] & 0 \\ 0 & \exp[-i\gamma_3(1)t] \end{pmatrix} \tag{82}$$

$$\begin{aligned} \begin{pmatrix} A_3(0) \\ A_4(0) \end{pmatrix} &= \mathbf{D}_{\mathrm{LR}}{}^{-1}(0)\mathbf{D}_{\mathrm{LR}}(1)\mathbf{P}_{\mathrm{LR}}(1)\mathbf{D}_{\mathrm{LR}}{}^{-1}(1)\mathbf{D}_{\mathrm{LR}}(0)\begin{pmatrix} A_3(2) \\ 0 \end{pmatrix} \\ &= \begin{pmatrix} \dfrac{1}{2}\left(1 + \dfrac{\sqrt{(n_y - ik_y)^2 - \sin^2\theta}}{\sqrt{n_0{}^2 - \sin^2\theta}}\right) & \dfrac{1}{2}\left(1 - \dfrac{\sqrt{(n_y - ik_y)^2 - \sin^2\theta}}{\sqrt{n_0{}^2 - \sin^2\theta}}\right) \\ \dfrac{1}{2}\left(1 - \dfrac{\sqrt{(n_y - ik_y)^2 - \sin^2\theta}}{\sqrt{n_0{}^2 - \sin^2\theta}}\right) & \dfrac{1}{2}\left(1 + \dfrac{\sqrt{(n_y - ik_y)^2 - \sin^2\theta}}{\sqrt{n_0{}^2 - \sin^2\theta}}\right) \end{pmatrix} \times \begin{pmatrix} \dfrac{1}{2}\left(1 + \dfrac{\sqrt{n_0{}^2 - \sin^2\theta}}{\sqrt{(n_y - ik_y)^2 - \sin^2\theta}}\right)\exp[i\gamma_3(1)t]A_3(2) \\ \dfrac{1}{2}\left(1 - \dfrac{\sqrt{n_0{}^2 - \sin^2\theta}}{\sqrt{(n_y - ik_y)^2 - \sin^2\theta}}\right)\exp[-i\gamma_3(1)t]A_3(2) \end{pmatrix} \\ &= \begin{pmatrix} \left\{\left(\dfrac{1}{2} + \dfrac{G}{4} + \dfrac{1}{4G}\right)\exp[i\gamma_3(1)t] + \left(\dfrac{1}{2} - \dfrac{G}{4} - \dfrac{1}{4G}\right)\exp[-i\gamma_3(1)t]\right\}A_3(2) \\ \left\{\left(\dfrac{G}{4} - \dfrac{1}{4G}\right)\exp[i\gamma_3(1)t] - \left(\dfrac{G}{4} - \dfrac{1}{4G}\right)\exp[-i\gamma_3(1)t]\right\}A_3(2) \end{pmatrix} \end{aligned} \tag{83}$$

where

$$G = \frac{\sqrt{n_0{}^2 - \sin^2\theta}}{\sqrt{(n_y - ik_y)^2 - \sin^2\theta}} \tag{84}$$

From eqs 4 and 5

$$1/T_s = \left|\left(\frac{1}{2} + \frac{G}{4} + \frac{1}{4G}\right)\exp[i\gamma_3(1)t] + \left(\frac{1}{2} - \frac{G}{4} - \frac{1}{4G}\right)\exp[-i\gamma_3(1)t]\right|^2 \tag{85}$$

$$1/R_s = \left|\frac{\left(\dfrac{1}{2} + \dfrac{G}{4} + \dfrac{1}{4G}\right)\exp[i\gamma_3(1)t] + \left(\dfrac{1}{2} - \dfrac{G}{4} - \dfrac{1}{4G}\right)\exp[-i\gamma_3(1)t]}{\left(\dfrac{G}{4} - \dfrac{1}{4G}\right)\exp[i\gamma_3(1)t] - \left(\dfrac{G}{4} - \dfrac{1}{4G}\right)\exp[-i\gamma_3(1)t]}\right|^2 \tag{86}$$

For p-polarized light in air

$$\gamma_1(0) = (\omega/c)\sqrt{n_0{}^2 - \sin^2\theta} \tag{87}$$

Thus

$$\mathbf{D}_{\mathrm{UL}}(0) = p_{11}(0)\begin{pmatrix} 1 & 1 \\ \dfrac{n_0{}^2}{\mu\sqrt{n_0{}^2 - \sin^2\theta}} & -\dfrac{n_0{}^2}{\mu\sqrt{n_0{}^2 - \sin^2\theta}} \end{pmatrix} \tag{88}$$

$$\mathbf{D}_{\mathrm{UL}}^{-1}(0) = \frac{1}{p_{11}(0)}\begin{pmatrix} 1/2 & \dfrac{\mu\sqrt{n_0{}^2 - \sin^2\theta}}{2n_0{}^2} \\ 1/2 & -\dfrac{\mu\sqrt{n_0{}^2 - \sin^2\theta}}{2n_0{}^2} \end{pmatrix} \tag{89}$$

where $p_{11}(0)$ is the value of p_{11} in the air as defined in eq 47.

For propagation in the film

$$\gamma_1(1) = (\omega/c)\frac{(n_x - ik_x)}{(n_z - ik_z)}\sqrt{(n_z - ik_z)^2 - \sin^2\theta} \tag{90}$$

Thus

$$\mathbf{D}_{\mathrm{UL}}(1) = p_{11}(1)\begin{pmatrix} 1 & 1 \\ \dfrac{(n_x - ik_x)(n_z - ik_z)}{\mu\sqrt{(n_z - ik_z)^2 - \sin^2\theta}} & -\dfrac{(n_x - ik_x)(n_z - ik_z)}{\mu\sqrt{(n_z - ik_z)^2 - \sin^2\theta}} \end{pmatrix} \tag{91}$$

$$\mathbf{D}_{\mathrm{UL}}{}^{-1}(1) = \frac{1}{p_{11}(1)}\begin{pmatrix} 1/2 & \dfrac{\mu\sqrt{(n_z - ik_z)^2 - \sin^2\theta}}{2(n_x - ik_x)(n_z - ik_z)} \\ 1/2 & -\dfrac{\mu\sqrt{(n_z - ik_z)^2 - \sin^2\theta}}{2(n_x - ik_x)(n_z - ik_z)} \end{pmatrix} \tag{92}$$

$$\mathbf{P}_{\mathrm{UL}}(1) = \begin{pmatrix} \exp[i\gamma_1(1)t] & 0 \\ 0 & \exp[-i\gamma_1(1)t] \end{pmatrix} \tag{93}$$

where $p_{11}(1)$ is the value of p_{11} in the film as defined in eq 47

$$\begin{pmatrix} A_1(0) \\ A_2(0) \end{pmatrix} = \mathbf{D}_{\mathrm{UL}}{}^{-1}(0)\mathbf{D}_{\mathrm{UL}}(1)\mathbf{P}_{\mathrm{UL}}(1)\mathbf{D}_{\mathrm{UL}}{}^{-1}(1)\mathbf{D}_{\mathrm{UL}}(0)\begin{pmatrix} A_1(2) \\ 0 \end{pmatrix}$$

$$= \begin{pmatrix} \frac{1}{2}\left(1 + \dfrac{(n_x - ik_x)(n_z - ik_z)\sqrt{n_0{}^2 - \sin^2\theta}}{n_0{}^2\sqrt{(n_z - ik_z)^2 - \sin^2\theta}}\right) & \frac{1}{2}\left(1 - \dfrac{(n_x - ik_x)(n_z - ik_z)\sqrt{n_0{}^2 - \sin^2\theta}}{n_0{}^2\sqrt{(n_z - ik_z)^2 - \sin^2\theta}}\right) \\ \frac{1}{2}\left(1 - \dfrac{(n_x - ik_x)(n_z - ik_z)\sqrt{n_0{}^2 - \sin^2\theta}}{n_0{}^2\sqrt{(n_z - ik_z)^2 - \sin^2\theta}}\right) & \frac{1}{2}\left(1 + \dfrac{(n_x - ik_x)(n_z - ik_z)\sqrt{n_0{}^2 - \sin^2\theta}}{n_0{}^2\sqrt{(n_z - ik_z)^2 - \sin^2\theta}}\right) \end{pmatrix} \times$$

$$\begin{pmatrix} \frac{1}{2}\left(1 + \dfrac{n_0{}^2\sqrt{(n_z - ik_z)^2 - \sin^2\theta}}{(n_x - ik_x)(n_z - ik_z)\sqrt{n_0{}^2 - \sin^2\theta}}\right)\exp[i\gamma_1(1)t]A_1(2) \\ \frac{1}{2}\left(1 - \dfrac{n_0{}^2\sqrt{(n_z - ik_z)^2 - \sin^2\theta}}{(n_x - ik_x)(n_z - ik_z)\sqrt{n_0{}^2 - \sin^2\theta}}\right)\exp[-i\gamma_1(1)t]A_1(2) \end{pmatrix}$$

$$= \begin{pmatrix} \left\{\left(\frac{1}{2} + \frac{H}{4} + \frac{1}{4H}\right)\exp[i\gamma_1(1)t] + \left(\frac{1}{2} - \frac{H}{4} - \frac{1}{4H}\right)\exp[-i\gamma_1(1)t]\right\}A_1(2) \\ \left\{\left(\frac{H}{4} - \frac{1}{4H}\right)\exp[i\gamma_1(1)t] - \left(\frac{H}{4} - \frac{1}{4H}\right)\exp[-i\gamma_1(1)t]\right\}A_1(2) \end{pmatrix} \tag{94}$$

where

$$H = \frac{n_0{}^2\sqrt{(n_z - ik_z)^2 - \sin^2\theta}}{(n_x - ik_x)(n_z - ik_z)\sqrt{n_0{}^2 - \sin^2\theta}} \tag{95}$$

From eqs 2 and 3

$$1/T_{\mathrm{p}} = \left|\left(\frac{1}{2} + \frac{H}{4} + \frac{1}{4H}\right)\exp[i\gamma_1(1)t] + \left(\frac{1}{2} - \frac{H}{4} - \frac{1}{4H}\right)\exp[-i\gamma_1(1)t]\right|^2 \tag{96}$$

$$1/R_{\mathrm{p}} = \left|\frac{\left(\frac{1}{2} + \frac{H}{4} + \frac{1}{4H}\right)\exp[i\gamma_1(1)t] + \left(\frac{1}{2} - \frac{H}{4} - \frac{1}{4H}\right)\exp[-i\gamma_1(1)t]}{\left(\frac{H}{4} - \frac{1}{4H}\right)\exp[i\gamma_1(1)t] - \left(\frac{H}{4} - \frac{1}{4H}\right)\exp[-i\gamma_1(1)t]}\right|^2 \tag{97}$$

References and Notes

(1) Elman, J. F.; Greener, J.; Herzinger, C. M.; Johs, B. *Thin Solid Films* **1998**, *313*−*314*, 814−818.
(2) Liu, T.; Samuels, R. *J. Polym. Sci. Part B: Polym. Phys.* **2001**, *39*, 2481−2490.
(3) Tammer, M.; Monkman, A. P. *Adv. Mater.* **2002**, *14*, 210−212.
(4) Losurdo, M.; Giangregorio, M. M.; Capezzuto, P.; Bruno, G.; Babudri, F.; Colangiuli, D.; Farinola, G. M.; Naso, F., *Macromolecules* **2003**, *36*, 4492−4497.
(5) Kirov, K. R.; Assender, H. E. *Macromolecules* **2004**, *37*, 894−904.
(6) Buffeteau, T.; Blaudez, D.; Pere, E.; Desbat, B. *J. Phys. Chem. B* **1999**, *103*, 5020−5027.
(7) Tompkins, H. G.; McGahan, W. A. *Spectroscopic Ellipsometry and Reflectometry A User's Guide*; John Wiley & Sons: New York, 1999.
(8) Woollam, J. A.; Bungay, C.; Hilfiker, J.; Wiwald, T. *Nucl. Instrum. Methods B* **2003**, *208*, 35−39.
(9) Parikh, A. N.; Allara, D. L. *J. Chem. Phys.* **1992**, *96*, 927−945.
(10) Yeh, P. *Optical Waves in Layered Media*; John Wiley & Sons: New York, 1988.
(11) Poelman, D.; Smet, P. F. *J. Phys. D-Appl. Phys.* **2003**, *36*, 1850−1857.
(12) Heminghaus, S.; Boese, D.; Yoon, D. Y.; Smith, B. A. *Appl. Phys. Lett.* **1991**, *59*, 1043−1045.
(13) Boses, D.; Lee, H.; Yoon, D. Y.; Swalen, J. D.; Rabolt, J. F. *J. Polym. Sci. Part B: Polym. Phys.* **1992**, *30*, 1321−1327.
(14) Lin, L.; Bidstrup, S. A. *J. Appl. Polym. Sci.* **1994**, 54, 553−560.
(15) Diao, J.; Hess, D. W. *Thin Solid Films* **2005**, *483*, 226−231.
(16) Diao, J.; Hess, D. W. *J. Phys. Chem. B* **2005**, *109*, 12819−12825.
(17) Lagarias, J. C., Reeds J. A.; Wright M. H.; Wright P. E. *SIAM J. Optimiz.* **1998**, *9*, 112−147.
(18) Hieptas, G. D.; Allara, D. L. *J. Polym. Sci. Part B: Polym. Phys.* **1998**, *36*, 1247−1260.
(19) Hieptas, G. D.; Sands, J. M.; Allara, D. L. *Macromolecules* **1998**, *31*, 3374−3378.